ORNL/TM-2005/90

# ANNUAL TECHNICAL PROGRESS REPORT OF RADIOISOTOPE POWER SYSTEM MATERIALS PRODUCTION AND TECHNOLOGY PROGRAM TASKS FOR OCTOBER 1, 2003 THROUGH SEPTEMBER 30, 2004

Prepared for Department of Energy
Office of Space and Defense Power Systems
Under Budget and Reporting Classification

AF 01 10 10 00, 40 04 13 00, 40 04 14 00,
40 04 16 00, and 40 04 03 30 05

by

Radioisotope Power System Program
Metals and Ceramics Division
Oak Ridge National Laboratory

Oak Ridge National Laboratory
Oak Ridge, Tennessee 37831-6080
Operated by UT-Battelle, LLC
for the
U. S. Department of Energy
Contract DE-AC05-00OR22725

CONTENTS

## 1.0 INTRODUCTION

The Office of Space and Defense Power Systems of the Department of Energy (DOE) provides Radioisotope Power Systems (RPS) for applications where conventional power systems are not feasible. For example, radioisotope thermoelectric generators were supplied by the DOE to the National Aeronautics and Space Administration for deep space missions including the Cassini Mission launched in October of 1997 to study the planet Saturn. For the Cassini Mission, ORNL produced carbon-bonded carbon fiber (CBCF) insulator sets, iridium alloy blanks and foil, and clad vent sets (CVS) used in the generators. The Oak Ridge National Laboratory (ORNL) has been involved in developing materials and technology and producing components for the DOE for more than three decades.

This report reflects program guidance from the Office of Space and Defense Power Systems for fiscal year (FY) 2004. Production and production maintenance activities for flight quality (FQ) CBCF insulator sets, iridium alloy blanks and foil, and CVS are summarized in this report. In all three cases, production maintenance is assured by the manufacture of limited quantities of FQ components. Technology activities are also reported that were conducted to improve the manufacturing processes, characterize materials, or to develop information for new radioisotope power systems.

## 2.0 PRODUCTION TASKS

## 2.1 CARBON-BONDED CARBON FIBER

### 2.1.1 Background

The CBCF production facilities have been operated in a production maintenance mode since the Cassini campaign to produce Flight Quality parts of insulation material. Dedicated facilities for CBCF production remain in the Carbon Materials Technology Laboratory of ORNL. CBCF sleeves produced in fiscal year 2000 were the first to be fully characterized as Flight Quality in nearly a decade. During much of the 1990s CBCF production was directed at making experimental variations of CBCF that explored the potential for improved insulating attributes at very high temperatures. The effect of brief excursions to reentry temperatures was also explored.

The impurity content of CBCF insulators produced in FY 2001 and FY 2002 had become an issue with respect to qualifying Flight Quality Insulators. Ca concentrations as high as 2500μg/g and Si concentrations as high as 510μg/g were found in some samples. The specification allowable is 200μg/g and 300μg/g, respectively. An extensive assessment of CBCF raw materials, procedures, processes and equipment was undertaken in FY 2003 to identify numerous opportunities for making CBCF having lower impurity content. An additional lot of Durez 22352 resin was purchased to the program specification in FY 2003. Although this resin is out of commercial production, Durez Corporation was able to produce a 200 lb quantity with the original specification raw materials using their pilot production facility. The new lot of resin was found to be dramatically lower in impurities when compared to the previous lot in use since 1990. Ca was several times lower and Si was two orders of magnitude lower.

Resolution of issues related to elevated impurities in CBCF allowed for the production of flight quality insulators in FY 2003. Thirteen Flight Quality CBCF Sleeves and more than forty Flight Quality CBCF Disks were produced.

### 2.1.2 CBCF Production in Fiscal Year 2004

Thirty-five CBCF Sleeves produced in FY 2002 and FY 2003 with impurity levels above the specification allowable were dispositioned for “Engineering Use” per NCR-CBCF-471. These sleeves meet all other property requirements.

An additional quantity of rayon fiber was chopped to support continued production of CBCF in FY 2005 and beyond. Approximately 614 pounds of Lot J-3634 rayon tow from North American Rayon Corp. was chopped to a nominal 0.38 mm length by Microfibers, Inc. in their Pawtucket, Rhode Island facility. This operation was carried out in accordance with Program Procedures and monitored by the CBCF Principal Technologist. Eight CBCF Flight Quality CBCF sleeves were produced for the acceptance of the new lot of chopped fiber.

A total of 16 additional Flight Quality Sleeves and 60 Flight Quality Disks were produced for future NASA missions. All insulators were produced with the new lot of resin qualified in FY 2003 and following measures established to enhance purity levels.

### 2.1.3 Material Recommendation for the GPHS Aeroshell

In response to a DOE directive of August 4, 2003 a GPHS Aeroshell Materials Working Group convened on three occasions to assess material options for the Aeroshell of the General Purpose Heat Source. The team made a broad survey of potential suppliers through a public Request for Information (RFI) procurement action. Two respondents offered carbon-carbon composites that are established reentry materials and could be considered as viable candidate materials under the current time constraints. A technical assessment of the two prime candidates was based on presentations by the vendors and performance modeling by working group members and their organizations. Issues related to cost, delivery and qualification were also considered.

### 2.1.4 Recommendation

*The overriding consensus of the GPHS Aeroshell Materials Working Group is that a reestablished FWPF represents the best choice of an Aeroshell material for future missions.* Although our information is imperfect, the impact modeling results of Orbital Sciences Corp. showing higher distortion in the clad for all velocities and orientations represents an obstacle to selecting the alternate composite material. The prospect of having that result confirmed after more modeling, testing, time and money would be formidable. Many aspects of the performance evaluation including reentry suggested that the alternate composite was an equivalent option but showed no distinct advantage over FWPF. The procurement cost and first delivery advantage of the alternate would be offset by the higher cost and time required for qualification. The assessment to date suggests a relatively low risk associated with restarting FWPF compared to a high risk associated with qualifying an alternative material. The current FWPF inventory at ANL-W, Textron and Lockheed Martin will be used for near term hardware/system qualifications and flights.

The analysis and discussions that evolved around the selection of a reestablished FWPF indicates that there is considerable potential for developing an improved material for the GPHS Aeroshell and Graphite Impact Shell to meet longer term requirements. For example, Textron could offer a 5D-FWPF material that represents a minor variation on the architecture of the currently specified 3D-FWPF material. By rotating alternate woven layers by 45º, the final composite will have more isotropic properties. The minimum circumferential strength of the Graphite Impact Shell would be substantially increased thereby providing greater constraint to the fueled clad. A few billets could be co-processed with the standard material for a small premium in cost per billet. High temperature properties required for modeling would be characterized. The broad selection of modern carbon fibers and varied architectures allows for the design and fabrication of a custom made carbon-carbon composite for the GPHS Aeroshell. The requirements and benefits of a custom made composite can be explored with existing

computer simulation. It is the further recommendation of the committee that a development effort be initiated to design, produce, evaluate and test enhanced materials for future missions.

## 2.2 IRIDIUM ALLOY BLANK AND FOIL PRODUCTION

The goals for this activity are to produce flight-quality blanks and foil under full configuration control, maintain production capability and to supply materials needed for clad vent set demonstration and maintenance activities. During FY 2004 a total of 160 flight-quality blanks were transferred to the CVS task. Data packages were prepared for a total of 61 pieces of foil. A total of 39 kg of iridium powder was purchased. A technician apprentice was hired and trained in melting and alloying. Iridium master alloys were produced and the applicable procedure was updated. Improvement to the a chemical analysis method was implemented as the result of trend analysis.

### 2.2.1 Iridium Powder Procurement and Certification

A total of 62 kg of iridium powder was received from the vendor in August 2003. Sampling and chemical analysis of the received powder by glow discharge mass spectrographic (GDMS) analysis showed that 23.4 kg of the powder did not to meet chemistry requirements. This was documented in NCR-21H-2145 in September 2003. About 12 kg of the powder was rejected for excessive sodium content of 320 ppm as compared to a specified maximum of 100 ppm, and about 11.4 kg was rejected for excessive silicon content of 100 to 120 ppm as compared to a specified maximum of 70 ppm. The powder was returned to vendor at the vendor's expense for replacement with new powder.

A total 23.4 kg of iridium powder was received from the vendor in December 2003 as a replacement for returned powder. A total of 8 kg of this powder failed to meet requirements for chemical analysis. The powder contained 81 to 102 μg/g (81 to 102 ppm) carbon. This exceeds the maximum concentration of 50 μg/g permitted by the specification. This lot also contains 120 to 330μg/g (120 to 330 ppm) sodium (Na). This exceeds the maximum concentration of 100 μg/g permitted by the specification. The nonconformance report NCR-21H-2146 was issued in January 2004 and the powder again returned for replacement. The 8 kg of powder was replaced in April 2004 and was found acceptable in receiving inspection.

A total of 36 kg of purchased iridium powder was received from the vendor in August 2004. One lot of about 11 kg contained 190 to 280 μg/g (190 to 280 ppm) sodium (Na) as analyzed by ORNL procedure. This exceeded the maximum concentration of 100 μg/g permitted by the specification. Another lot of about 4.6 kg contains 89 to 92 μg/g (89 to 92 ppm) ruthenium (Ru) as analyzed by ORNL procedure. This exceeded the maximum concentration of 50 ppm permitted by the specification. These two lots of powder were documented by NCR-21H-2151 issued in August 2004 and returned to the vendor. Replacement powder was received and is currently being sampled for chemical analysis.

An additional 3 kg of powder was purchased during FY 2004 using funds from another program. This powder was in exchange for iridium alloy scrap material provided to that program. The material was found to contain 62 µg/g of Ru as compared to the specification requirement of 50 µg/g maximum. This powder was accepted for use as-is under NCR IRB&F 2150.

A total of 52-kg of the purchased powder was designated for the K-batch. The powder was screened, weighed, and blended to produce 18 batch blends of about 2.9 kg each. The remaining purchased powder was stored for future use in an L-batch powder.

2.2.2 Blank Production

The G5 extrusion produced in the previous year was processed to produce blanks. The molybdenum can was chemically removed from the G5 extruded bar. A total of 17 rolled sheets were prepared from the extruded bar. A total of 111 blanks were electro-discharge machined from these sheets and ground to final thickness. All of these blanks passed dimensional inspection. All but two blanks from ingot G5 passed ultrasonic inspection. These two blanks together with one additional blank will be used for tensile impact testing and weldability testing. All blanks passed dye penetrant inspection. Chemical analyses and metallographic inspections were successfully completed. A total of 19 blanks were reworked by sanding to remove indications of visual indications of defects in accordance with approved procedures. The reworked blanks passed all inspections.

A total of 57 prime blanks from ingot G5 sheets 1 through 11 were transferred to the CVS task on May 20, 2004. A total of 33 prime blanks from G5 ingot, sheets 12 through17 were transferred to the CVS task on June 29, 2004. A total of 19 reworked blanks from G5 ingot were transferred the CVS task together with and approved data package on August 18, 2004.

The G6 ingot was fabricated and processed to blanks. A total of 17 kg of G-batch powder was prepared as six batch blends of about 2.9 kg each. The blended Ir – 0.3% W powder was compacted, sintered in hydrogen gas, and vacuum outgassed. The compacts were electron-beam melted to produce 30 alloy buttons. The buttons were non-consumable arc melted in argon, alloyed with thorium and aluminum master alloy and drop-cast to produce DOP-26 alloy electrode segments for the G6 ingot. The segments were electron beam welded to produce the G6 electrode. The electrode was vacuum arc remelted to produce the G6 ingot. The ingot was placed in a molybdenum can and hot extruded. The extrusion can was removed and the extrusion sectioned and rolled to produce 15 sheets. A total of 107 blanks were electro-discharge machined from these sheets and ground. All but three blanks passed dimensional inspection. The blanks were cleaned and stress relieved. Nondestructive examination and chemical and metallographic analysis are planned to complete in November 2004.

The G8 ingot was fabricated and extruded. A total of 17 kg of G-batch powder was prepared as six batch blends of about 2.9 kg each. The blended Ir – 0.3% W powder was

compacted, sintered in hydrogen gas, and vacuum outgassed. The compacts were electron-beam melted to produce 30 alloy buttons. The buttons were non-consumable arc melted in argon, alloyed with thorium and aluminum master alloy and drop-cast to produce DOP-26 alloy electrode segments for the G8 ingot. The segments were electron beam welded to produce the G8 electrode. The electrode was vacuum arc remelted to produce the G8 ingot. The ingot was placed in a molybdenum can and hot extruded. The extrusion can was removed. Traveler documents have been issued for processing to blanks.

Processing of K-batch powder to produce the K1 ingot was initiated. Six batch blends, K-1 through K-6, are being processed for this ingot. The powder was blended with tungsten powder, compacted, sintered vacuum outgassed. The compacts were electron-beam melted to produce button of Ir-0.3% W alloy. Alloying and drop-casting of the K1 electrode segments was begun.

Processing of K-batch powder to produce the K2 ingot was also initiated. Six batch blends, K-7 through K-12, are being processed for this ingot. About one half of this powder was blended and compacted.

### 2.2.3 Foil Production

Four electron-beam melted buttons from G-batch material and recycle material from several batches were used as starting stock for foil ingots GFR241 through GFR246. The starting materials were weighed and cleaned and button arc melted and drop-cast to produce the six small ingots of 19-mm square by 55-mm high. The ingots were homogenized and rolled to 0.22 mm with cleaning and in-process recrystallization at gauge thickness of 6-mm and 0.7-mm. The foil was then cleaned and rolled to final thickness. The foils were dimensionally inspected, cleaned and recrystallized. Samples were subjected to metallographic examination and chemical analysis by combustion methods for carbon and oxygen and by GDMS for alloying and impurity elements. All foils met the requirements of the foil specification. Data packages have been prepared.

### 2.2.4 Master Alloy Production

Master alloys of Ir-0.3%-W – 2% Th and Ir-0.3%-W – 2% Al are used for alloying during the button arc melting of material for blanks and foil. Under SIDR-Ir-80 a total of about 200 grams of nominal Ir-2% Th master alloy (MT-14) and 200 grams of nominal Ir-2% Al master alloy (MA-13) was produced using a draft revision 3 of procedure MET-MatP-SOP-90. The fabrication of the alloys was the same as in the previous rev.2 of the procedure with some additional instructions for ES&H practices. The chemical analyses of the Th and Al master alloys by the isotope dilution and Paschen methods respectively were not performed. Instead the master alloy materials were used to make two buttons of DOP-26 alloy of about 1000 grams each. The chemistry of the two buttons was analyzed using approved analytical methods and the analysis showed that specification requirements for chemistry were met and thorium and aluminum levels in the buttons were normal. The SIDR was approved permitting use of the master alloy for future production and also use of the DOP-26 alloy buttons. On the basis of the above results the draft revision of the procedure MET-MatP-SOP-90 was approved as revision 3 for routine use as DR-Ir-211.

2.2.5 Transfers of Materials to CVS Production Task

A total of 27 blanks from ingots G2, G1, and ER8 were transferred to the CVS task on March 16, 2004. A total of 22 blanks from ingots ER10 and 12 blanks from AR2 were transferred to the CVS task on May 4, 2004. A total of 18 pieces of foil from ingots GFR235 and 236, with weight of 475 g and area of 0.165 square meters, were transferred to CVS task on June 21, 2004.

2.2.6 Training

A technician apprentice was hired and trained in button arc melting and drip-casting of iridium alloys. The apprentice is to replace the technician who previously performed this task and who had suddenly left the Laboratory. A technician on temporary assignment from the Oak Ridge Y-12 Plant for six months was also trained in this operation. Two other technicians were trained in operation of the equipment for button arc melting, although without the specific qualification for melting of iridium alloys. A third machinist was trained in the grinding of iridium alloy blanks

2.2.7 Production Equipment

An equipment malfunction during the consumable arc melting of GR7 electrode resulted in copper contamination of the ingot. The electrode contained 14 kg of iridium alloy recycle material. The cause of the contamination is documented in NCR IRB&F 2148 as a loss of the current measurement signal to current controller and digital current indicator, resulting in actual melting currents above the value called for in the procedure. One corrective action is that operator and task leader are aware to promptly abort a melt in the event of any abnormality during the melting time of about 3 minutes. The equipment failure mode could not be reproduced during the subsequent melting of six stainless steel electrodes or on Nb-1Zr alloy electrode. An on-site visit by the furnace manufacturer's service representative did not find any defect in the control system and no repairs were made. A quotation for a new and updated furnace control system was obtained for consideration as a future capital equipment acquisition. The determination of what material from the GR7 ingot may be acceptable for recycling is in progress under revision 1 of the above NCR.

A purchase order was placed for a new 16 x 16 x 48 inch tungsten metal hot zone for an existing high temperature vacuum annealing furnace. The furnace located at the Oak Ridge Environmental Technology Park (K-25 site) will be relocated to the Materials Processing group laboratory at ORNL. The existing hot zone has been removed from the furnace and those hot zone components that are reusable are being saved. Relocation of the furnace and installation of the hot zone are planned to be completed in March 2005. It is planned that this will become the primary annealing furnace for iridium alloy blank and foil processing.

2.2.8 Trend Analysis For Iridium Alloy Blank And Foil Production

Trending analysis was performed for dimensional, nondestructive evaluations for blanks for the period FY2001 through FY2003. Trend analysis was also performed on chemical

analysis of blanks and foil for FY2001 through the first half of FY2004. The trend analysis of GDMS chemistry reports led to further studies and a procedure change, which are also described below.

2.2.8.1 Trend analysis of dimensional measurements

The results of the thickness inspections are listed in Table 1 for blanks processed from each production ingot since 1999. The ingots are listed in chronological order. The thickness is measured at a minimum of seven locations on each blank and a maximum and minimum value is reported. The distribution of the minimum thickness values is shown as the percentage of all blanks from the ingot at each increment of minimum thickness value from 0.62 to 0.68 mm. Each of the three ingots had one blank (1% of all blanks) that was rejected for a thickness value of less than 0.62 mm. The experience in clad vent set (CVS) production favors having a narrow distribution of thickness values with the average thickness above 0.66 mm and minimum thickness values preferably of 0.65 mm or greater. This minimizes the chances of cups with thickness values in the weld zone less than the required 0.63 mm.

Similar analyses of blank thickness measurements for ingots used for Cassini production are shown in Table 2. The results of thickness measurements for recent blanks in Table 1 are comparable to those for the latter part of the Cassini production. For each of the three recent ingots no more than 10% of blanks are outside the range of 0.65 to 0.67 mm minimum thickness. In addition the variation in thickness measured within each blank is no more than 0.01 mm.

During the grinding of blanks from G2 ingot in 1999 it was observed that greater than usual variations in thickness were occurring. This was attributed to the grinding of the vacuum chuck over a period of many years, which reduced the depth of the slots in the chuck resulting in reduced hold down force on the blanks. A revision in the procedure in 2001 added a requirement for a minimum slot width in the vacuum chuck prior to proceeding with the grinding of blanks. This has been effective for blanks ground since that time.

In addition eight blanks from ingot G3 and four blanks from ingot GR4 failed to clean up during grinding. This can be attributed in part to the remaining curvature in the sheets after straightening, in part to the residual stresses remaining after the stress relief treatment of the sheets, and in part to the grinding technique. Any major variation in surface roughness is invariably related to failure of the grinding to clean up the surface before the minimum blank thickness is achieved.

The diameter measurements for all blanks from the G3 ingot were within the range of 52.10 to 52.29 mm. The diameter measurements for all blanks from the GR4 ingot were within the range of 52.06 to 52.29 mm. The specification for blank diameter is 51.80 to 52.35 mm. Essentially all measurements of diameter for all blanks from the two ingots are in the upper half of the range of acceptable diameter values.

**Table 1. Distribution of minimum thickness values of blanks by ingot for recent (post-Cassini) production**

| | Percentage of blanks with listed minimum thickness, mm | | | | | | |
|---|---|---|---|---|---|---|---|
| Ingot | 0.62 | 0.63 | 0.64 | 0.65 | 0.66 | 0.67 | 0.68 |
| G2 | 0 | 0 | 10 | 28 | 48 | 14 | 0 |
| G3 | 0 | 0 | 1 | 14 | 35 | 43 | 7 |
| GR4 | 0 | 2 | 3 | 27 | 57 | 11 | 0 |

**Table 2. Distribution of minimum thickness values of blanks by ingot for Cassini production**

| | Percentage of blanks with listed minimum thickness, mm | | | | | | |
|---|---|---|---|---|---|---|---|
| Ingot | 0.62 | 0.63 | 0.64 | 0.65 | 0.66 | 0.67 | 0.68 |
| E1 | 0 | 0 | 6 | 38 | 56 | 0 | 0 |
| CR3 | 0 | 0 | 9 | 31 | 54 | 5 | 0 |
| E2 | 0 | 1 | 2 | 38 | 51 | 7 | 0 |
| D2 | 2 | 16 | 29 | 31 | 19 | 3 | 0 |
| E3 | 0 | 4 | 23 | 36 | 33 | 3 | 0 |
| CR4 | 4 | 19 | 27 | 31 | 18 | 0 | 0 |
| E4 | 4 | 13 | 31 | 37 | 16 | 0 | 0 |
| ER6 | 5 | 15 | 16 | 26 | 26 | 12 | 0 |
| DR3 | 1 | 2 | 5 | 41 | 51 | 1 | 0 |
| ER7 | 0 | 0 | 0 | 27 | 66 | 7 | 0 |
| ER8 | 0 | 2 | 7 | 33 | 57 | 1 | 0 |
| F1 | 0 | 0 | 11 | 38 | 36 | 16 | 0 |
| E5 | 0 | 1 | 2 | 8 | 71 | 18 | 0 |
| F2 | 0 | 1 | 3 | 23 | 54 | 19 | 0 |
| ER9 | 0 | 0 | 0 | 2 | 36 | 62 | 0 |
| FR3 | 0 | 0 | 0 | 4 | 41 | 55 | 0 |
| G1 | 0 | 0 | 5 | 27 | 60 | 8 | 0 |

2.2.8.2 Trend Analysis of Nondestructive Inspection of Blanks

The results of nondestructive examination of blanks are shown in Table 3 for FY 2001 through FY 2003. With the exception of one blank from G3 ingot and two blanks from GR4 ingot that failed ultrasonic inspection, all nonconformances were due to indications of inclusions in the visual inspection. All of the blanks with indications of inclusions were reworked by sanding in accordance with an approved procedure and were acceptable upon reinspection. A total of 13% of blanks from the G3 ingot required rework as compared to 18% of the blanks from the GR4 ingot. In the cases of both ingots there were large variations between contiguous runs of blanks in the percentage of blanks that passed the inspection. The contiguous run consists of up to six sheets from the same ingot, which are processed as a group through the rolling and machining processes.

No microanalysis was performed on any of the inclusions found on the blanks from ingots G3 or GR4. Previous analyses of inclusions on the surfaces of ground blanks have typically found the inclusions to contain aluminum and silicon, presumably present as oxides. The results suggest that the inclusions are not present in the melted ingot but rather become embedded in the surface of the sheet during the processing. If the inclusions were in the melt the numbers of blanks passing the visual inspection would not be expected to show such large changes between the contiguous runs of sheets from the same ingot. The grinding of the blanks typically removes 0.1 mm or more from each side. Since the rolled surface is essentially removed during the grinding of the blanks, the introduction of oxide particles to the surface of the blanks is likely due to the grinding operation itself rather than the rolling of the sheets. Variations in the number of inclusions on the surface of the blanks may be the result of small changes in grinding technique.

**Table 3. Results of Nondestructive Examination of Blanks**

| Ingot | Sheets | Date | No. inspected | # passed | % passed |
|---|---|---|---|---|---|
| G3 | 1-6 | June-01 | 32 | 31 | 97 |
| G3 | 7-16 | August-02 | 53 | 43 | 81 |
| GR4 | 1-5 | October-02 | 30 | 12 | 40 |
| GR4 | 6-11 | January-03 | 35 | 34 | 97 |
| GR4 | 12-17 | March-03 | 36 | 35 | 97 |

2.2.8.3 Trending of Chemical Analysis Results

Chemical analysis for alloying elements and impurities, other than carbon and oxygen are performed by glow discharge mass spectrography. Currently the analyses are performed by Shiva Technologies Inc. (Syracuse NY) in accordance with procedure MET-MatP-SOP-79. The procedure and the laboratory were approved by a deviation request (DR-Ir-206) on June 3, 2002. This procedure makes use of two reference materials supplied by ORNL and run with each group of up to ten test samples.

The results for alloying and impurity elements for ingot G3 are shown in Table 4. These analyses were all reported in August 2002. The reference pin identities for these analyses were G1-10-4 and RS10-9-53. The results for alloying and impurity elements for ingot GR4 are shown in Table 5. The dates of the analyses and identities of the reference pins are shown in the table for each of the analyses. The results for alloying and impurity elements for foil ingots GFR231 through GFR236 are shown in Table 6. These analyses were all reported in August 2002. The reference pin identities for these analyses were G1-10-3 and RS10-9-51.

**Table 4. Chemical Analysis of G3 Ingot Materials**

| Element | Composition measured by Glow Discharge Mass Spectrograph, ppm by weight | | | | | |
|---|---|---|---|---|---|---|
| | Sheet Number | | | | | |
| Element | G3-7 | G3-9 | G3-11 | G3-13 | G3-15 | Std dev. |
| Al | 49 | 49 | 46 | 48 | 47 | 1.3 |
| Si | 2.3 | 2.5 | 2.3 | 2.4 | 2.6 | 0.1 |
| Ti | 1.8 | 1.7 | 1.7 | 1.8 | 2 | 0.1 |
| Cr | 0.1 | 0.13 | 0.13 | 0.15 | 0.22 | 0.0 |
| Fe | 0.43 | 0.42 | 0.43 | 0.46 | 0.95 | 0.2 |
| Ni | 0.13 | 0.13 | 0.13 | 0.14 | 0.14 | 0.0 |
| Cu | 0.71 | 0.28 | 0.31 | 0.34 | 0.3 | 0.2 |
| Nb | 0.76 | 0.79 | 0.73 | 0.77 | 0.9 | 0.1 |
| Mo | 1.6 | 1.4 | 1.5 | 1.7 | 1.8 | 0.2 |
| Ru | 17 | 17 | 17 | 18 | 17 | 0.4 |
| Rh | 3.7 | 4.1 | 3.9 | 3.8 | 3.8 | 0.2 |
| Ta | 4.5 | 4.4 | 4.4 | 4.6 | 4.3 | 0.1 |
| W | 2720 | 2720 | 2620 | 2810 | 2720 | 67 |
| Pt | 4.2 | 4.5 | 4.5 | 4.2 | 4.5 | 0.2 |
| Th | 57 | 53 | 51 | 59 | 53 | 3.3 |

**Table 5. Chemical Analysis of GR4 Ingot Materials**

| | Composition measured by Glow Discharge Mass Spectrograph, ppm by weight | | | | | |
|---|---|---|---|---|---|---|
| | Sheet Number | | | | | |
| Element | GR4-1 | GR4-3 | GR4-5 | Std. Dev All GR4 | | |
| Al | 41 | 35 | 38 | 3.9 | | |
| Si | 3.7 | 3.1 | 3.8 | 0.5 | | |
| Ti | 2.3 | 2.4 | 2.5 | 0.1 | | |
| Cr | 0.48 | 0.55 | 0.46 | 0.1 | | |
| Fe | 2.4 | 2.5 | 2 | 0.3 | | |
| Ni | 0.4 | 0.41 | 0.35 | 0.0 | | |
| Cu | 0.25 | 0.11 | 0.13 | 0.1 | | |
| Nb | 1.7 | 1.5 | 2.1 | 0.3 | | |
| Mo | 6.5 | 3.3 | 3.7 | 1.1 | | |
| Ru | 17 | 17 | 18 | 1.1 | | |
| Rh | 3 | 2.8 | 3.2 | 0.3 | | |
| Ta | 3.9 | < 1 | 4.3 | 0.2 | | |
| W | 3070 | 3070 | 3070 | 137 | | |
| Pt | 3.6 | 3.4 | 3.9 | 0.4 | | |
| Th | 77 | 78 | 82 | 6.5 | | |
| Date | 25-Nov-02 | 25-Nov-02 | 25-Nov-02 | | | |
| ref. pin 1 | G1-10-4 | G1-10-4 | G1-10-4 | | | |
| ref. pin 2 | RS10-9-52 | RS10-9-52 | RS10-9-52 | | | |
| | | | | | | |
| Al | 43 | 38 | 45 | 45 | 41 | 47 |
| Si | 2.7 | 2.7 | 3.7 | 3.4 | 2.7 | 4 |
| Ti | 2.1 | 2.1 | 2.3 | 2.3 | 2.4 | 2.5 |
| Cr | 0.4 | 0.42 | 0.4 | 0.5 | 0.46 | 0.53 |
| Fe | 1.6 | 1.8 | 1.7 | 2.1 | 2.3 | 2.3 |
| Ni | 0.35 | 0.37 | 0.37 | 0.42 | 0.4 | 0.41 |
| Cu | 0.12 | 0.14 | 0.13 | 0.17 | 0.18 | 0.24 |
| Nb | 1.6 | 1.8 | 1.9 | 2.1 | 2.2 | 2.5 |
| Mo | 3.3 | 3.1 | 2.8 | 3.3 | 3.8 | 4.5 |
| Ru | 15 | 16 | 16 | 18 | 17 | 18 |
| Rh | 2.6 | 2.5 | 2.3 | 2.8 | 2.7 | 2.9 |
| Ta | 4 | 4.3 | 4 | 4.2 | 4.2 | 4.3 |
| W | 2870 | 2750 | 2800 | 3010 | 2840 | 3100 |
| Pt | 3.3 | 3 | 3.6 | 2.8 | < 0.05 | 3.2 |
| Th | 66 | 63 | 77 | 66 | 70 | 73 |
| Date | 26-Feb-03 | 26-Mar-03 | 26-Feb-03 | 26-Mar-03 | 26-Mar-03 | 26-Mar-03 |
| ref. pin 1 | G1-10-6 | G1-10-6 | G1-10-6 | G1-10-6 | G1-10-6 | G1-10-6 |
| ref. pin 2 | RS10-9-6 | RS10-9-6 | RS10-9-6 | RS10-9-6 | RS10-9-6 | RS10-9-6 |

The results for the G3 ingot all fall within a narrow range. The standard deviations in the measured values are small and the alloying element compositions are all near the aim composition of 50 ppm Al, 3000 ppm W, and 60 ppm Th. The results for the GR4 material performed at three different times show greater standard deviations for the alloying elements Al, W, and Th than do the results for G3. The standard deviation for thorium results for the GR4 samples is 10% of the mean value. The standard deviations are even higher for the foil analyses shown in Table 6. The thorium results have a standard deviation of 30% of the mean thorium value. Most recently analysis of nine samples from ingot G5 in April 2004 showed an average of 56 ppm thorium with a standard deviation of 4 ppm, or a relative standard deviation of 0.07.

It seems likely that the variation in measured thorium values is due to the variability in the measurement technique rather than to variations in the samples themselves. This is deduced by comparing the results from the two reference pins that are run with each group of test samples. Table 7 is a comparison of the thorium contents reported for the two reference pins used for each group of analyses. The ratio of the thorium for the two reference materials should be constant, to the extent that the reference materials are uniform. The uniformity of the reference materials has been characterized previously and is shown in Table 6 as the standard deviation for the G1-10 and RS10-9 reference material. The standard deviation in the ratio of the two reference materials is shown in the right column and can be compared to the pooled standard deviation of the two reference materials. In the case of thorium, the standard deviation in the ratio of the thorium contents between the reference materials is nearly 5 times what would be expected based on the previously measured variability in the reference materials themselves. In contrast, the standard deviations in the ratio of the aluminum and tungsten values for the two reference materials are about what would be expected based on the pooled variance of the reference materials.

2.2.8.4 Trending of Chemical Analysis of Reference Materials

Due to the variability seen in the analyzed thorium content of described above as well as some samples from clad vent sent manufacturing a review was conducted of the data reported for the standard pins with each group of samples or job. A total of nine pin samples of the G1-10 standard material were analyzed as a group within a single day. Seven of these pins had been analyzed previously and had been returned to ORNL after use as standards. Two pins identified as G1-11 and G1-12 had been analyzed previously. One of the objectives of this study was to determine if repeated analysis of the same pin results in a consistent trend in the GDMS results. During analysis some material is removed from the pin and the shape and thickness of the pin does change over time, potentially having an effect on the analytical results.

All samples were prepared and cleaned at ORNL and analyzed in accordance with the standard procedure. Both “uncorrected results” and “corrected results” are reported. The uncorrected results are obtained from the raw data and a list of relative sensitivity factors which are maintained by Shiva. The corrected results are obtained as ratios of the uncorrected results to those of the standard pins run with each job. Corrected results are

obtained for the alloying elements Th, Al, and W using a G1-10 standard pin. Corrected results are obtained for 12 important impurity elements using a RS10-9 standard pin. The standard pin is 0.65 by 2 mm in cross section and 20 mm in length. Material removal rate during glow analysis average 0.35 micrometer/min, although edges and corners experience above average removal rates.

The results of the alloying elements thorium, aluminum, and tungsten analyses for various G1-10 standard pins over the past 30 months are listed in Table 8. These results for bulk analysis are "uncorrected" and cannot be compared directly to the specification limits for thorium. In each case there is no consistent trend in the analytical results such as would be expected if changes in the shape of the pin caused by repeated analysis of the same pin were a primary source of variation in the analytical results.

**Table 6. Chemical Analysis of GFR Ingot Foils**

Composition by Glow Discharge Mass Spectrograph, ppm by weight

| Element | 231 | 232 | 233 | 234 | 235 | 236 | Std. dev. |
|---|---|---|---|---|---|---|---|
| Al | 69 | 63 | 57 | 50 | 50 | 69 | 9 |
| Si | 3.2 | 2.8 | 3.5 | 3.5 | 2.7 | 3.9 | 0.5 |
| Ti | 3.3 | 2.9 | 2.1 | 2 | 2.7 | 3 | 0.5 |
| Cr | 2.8 | 1.3 | 1.1 | 3.8 | 1.4 | 4.2 | 1.4 |
| Fe | 5.5 | 4.9 | 4.4 | 15 | 5 | 15 | 5 |
| Ni | 1.7 | 1.5 | 1.4 | 3.3 | 2.5 | 3.6 | 1.0 |
| Cu | 0.92 | 0.97 | 1 | 1.5 | 0.85 | 1.4 | 0.3 |
| Nb | 0.96 | 0.96 | 0.69 | 0.47 | 0.88 | 0.76 | 0.2 |
| Mo | 7.7 | 7.7 | 5.7 | 3.3 | 6.4 | 5.6 | 2 |
| Ru | 23 | 22 | 18 | 18 | 20 | 24 | 3 |
| Rh | 8.8 | 7.5 | 7.5 | 7.5 | 6.7 | 9.5 | 1.0 |
| Ta | 3.9 | 3.7 | 4.2 | 3.7 | 3 | 3.2 | 0.4 |
| W | 2550 | 2630 | 2100 | 2250 | 2250 | 2630 | 229 |
| Pt | 5.2 | 4.3 | 6.2 | 4.6 | 4.9 | 4.7 | 0.7 |
| Th | 25 | 22 | 11 | 12 | 20 | 22 | 6 |

**Table 7. Analyses of Iridium Alloy Reference Materials**

| Element | Mean concentration G1-10 | Mean concentration RS10-9 | Relative Std. Dev. In G1-10, % | Relative Std. Dev. In RS10-9, % | Pooled Rel. Std. Dev.% | Std. Dev of Ratio G1-10 /RS10-9, % |
|---|---|---|---|---|---|---|
| Al | 50 | 53 | 3 | 8 | 9 | 11 |
| Si | 1.8 | 3.4 | 4 | 12 | 13 | 18 |
| Ti | 1.9 | 3.5 | 6 | 3 | 7 | 13 |
| Cr | 0.2 | 5.7 | 10 | 5 | 11 | 9 |
| Fe | 0.8 | 22 | 10 | 5 | 11 | 19 |
| Ni | 0.1 | 4.1 | 25 | 11 | 27 | 9 |
| Cu | 0.4 | 0.7 | 17 | 28 | 33 | 24 |
| Nb | 0.3 | 37 | 10 | 3 | 10 | 11 |
| Mo | 1 | 27 | 3 | 5 | 6 | 9 |
| Rh | 3 | 3.8 | 3 | 5 | 6 | 10 |
| Ta | 2.7 | 7.1 | 14 | 5 | 15 | 22 |
| W | 3000 | 3230 | 4 | 3 | 5 | 8 |
| Pt | 3.5 | 3 | 6 | 6 | 8 | 24 |
| Th | 60 | 55 | 3 | 3 | 4 | 19 |

**Table 8. Historical Summary of GDMS Data for G1-10 Reference Pins at Shiva**

| job # | date | run # | pin ID | Th, ppm | Al, ppm | W, ppm |
|---|---|---|---|---|---|---|
| UK3027 | 11/28/01 | U01112010 | G1-10-1 | 47 | 98 | 4300 |
| UK3027 | 11/28/01 | U01112015 | G1-10-2 | 44 | 110 | 4600 |
| UK3027 | 11/28/01 | U01112010A | G1-10-1 | 52 | 100 | 4500 |
| UL0208 | 2/5/02 | U02012559 | G1-10 | 40 | 100 | 4800 |
| UL2115 | 8/2/02 | U02080104 | G1-10-3 | 43 | 79 | 4000 |
| UL0536 | 3/13/02 | U02030109 | G1-10-3 | 44 | 85 | 4400 |
| UL2179 | 8/15/02 | U02080808 | G1-10-4 | 27 | 64 | 3100 |
| UL2322 | 8/28/02 | U02082306 | G1-10-4 | 43 | 80 | 4200 |
| UL3190 | 11/25/02 | U021114045 | G1-10-4 | 35 | 84 | 3600 |
| UL3551 | 1/2/03 | U021220031 | G1-10-4 | 28 | 93 | 3950 |
| UM0480 | 2/26/03 | U030218043 | G1-10-6 | 38 | 79 | 4300 |
| UM0762 | 3/26/03 | U030314012 | G1-10-6 | 36 | 100 | 3500 |
| UM1161 | 4/21/03 | U030414027 | G1-10-6 | 28 | 100 | 4000 |
| UM1419 | 5/14/03 | U030507007 | G1-10-7 | 34 | 83 | 3800 |
| UM2832 | 9/15/03 | U030902039 | G1-10-8 | 30 | 100 | 3300 |
| UM3074 | 9/26/03 | U030923004 | G1-10-8 | 28 | 83 | 2700 |
| UM4225 | 12/16/03 | U031211043 | G1-10-9 | 18 | 73 | 4500 |

| | | | | | | |
|---|---|---|---|---|---|---|
| UN0688 | 3/2/04 | U040225010 | G1-10-10 | 32 | 65 | 4000 |
| UN1210 | 4/7/04 | U040402017 | G1-10-10 | 33 | 73 | 4500 |
| UN1387 | 4/25/04 | U040416072 | G1-10-10 | 34 | 94 | 4200 |
| UN1498 | 4/27/04 | U040423036 | G1-10-10 | 33 | 79 | 4300 |
| UN1651 | 5/6/04 | U040505023 | G1-10 | 36 | 70 | 4000 |
| UN1651 | 5/6/04 | U040505024 | G1-10-3 | 36 | 80 | 4700 |
| UN1651 | 5/6/04 | U040505025 | G1-10-4 | 28 | 91 | 4200 |
| UN1651 | 5/6/04 | U040505026 | G1-10-6 | 29 | 82 | 4200 |
| UN1651 | 5/6/04 | U040505027 | G1-10-7 | 29 | 78 | 4000 |
| UN1651 | 5/6/04 | U040505028 | G1-10-8 | 28 | 73 | 4100 |
| UN1651 | 5/6/04 | U040505029 | G1-10-9 | 23 | 80 | 4100 |
| UN1651 | 5/6/04 | U040505022 | G1-10-11 | 23 | 85 | 4000 |
| UN1651 | 5/6/04 | U040505030 | G1-10-12 | 20 | 69 | 4000 |
| mean | | | | 33 | 84 | 4062 |
| rel.stdev. | | | | 0.24 | 0.14 | 0.11 |

2.2.8.5 Effect of Pin Length on Thorium Analysis by GDMS

The pin length and corresponding measured Th contents for G1-10 pins is shown in Table 9. The measured uncorrected thorium values are plotted versus pin length in Figure 1. A linear regression analysis shows a strong correlation between pin length and analyzed thorium content over the range of pin lengths of 17.3 mm to 20 mm. An adjustment value can be calculated from the linear regression analysis. This adjustment value is added to the measured thorium content. The adjustment value is by definition zero for a pin of 20 mm and increases with decreasing pin length. The adjustment values and adjusted Th concentrations are shown in the third and fourth column of Table 1. The average concentration, standard deviations, variances are tabulated for both the measured Th concentrations and the adjusted concentrations. The relative standard deviations are shown as the ratio of the standard deviation to the average value. In both cases using a corrected value of 60 ppm Th for this material, which is its reference concentration, a corrected standard deviation in ppm Th is calculated by multiplying the relative standard deviation by 60 ppm.

Analysis of the variance indicates that 85% of the variance in measured Th contents is attributable to variation in pin length. The relative standard deviation in the adjusted Th concentration of 0.056 (5.6%) is somewhat greater than the value of 0.03 (3%) measured previously at ORNL on a small sample size over a limited time period, but is still quite reasonable.

This conclusion of trend analysis is that the tolerance on pin length should be much smaller than that previously permitted. The deviation request Ir –212 has been approved

to specify pin length of 20.0 ± 0.3 mm on pin length for the sample preparation procedures and GDMS analysis procedure. In addition Shiva Technologies has been advised of the need to maintain the specified range of distance between the end of the pin and the cell exit slit of 9.5 plus or minus 0.5 mm as a maximum a variation. This variation in distance corresponds to an uncertainty in thorium content of 2.7 ppm.

**Table 9. Effect of Adjusting Th Content Based on Measured Pin Length**

| | Uncorrected Values of Thorium | | |
|---|---|---|---|
| pin length | measured | adjust value* | adjust conc. |
| mm | Th ppm | ppm | Th ppm |
| 20 | 36 | 0.0 | 36.0 |
| 19.5 | 36 | 2.7 | 38.7 |
| 17.7 | 28 | 12.5 | 40.5 |
| 18 | 29 | 10.9 | 39.9 |
| 18.2 | 29 | 9.8 | 38.8 |
| 18.2 | 28 | 9.8 | 37.8 |
| 17.3 | 23 | 14.7 | 37.7 |
| 17.5 | 23 | 13.6 | 36.6 |
| 17.5 | 20 | 13.6 | 33.6 |
| average | 28.0 | 37.8 | |
| std dev | 5.5 | 2.1 | |
| variance | 30.5 | 4.5 | |
| rel.std dev | 0.197 | 0.056 | |

| | Corrected Average Values of Thorium | |
|---|---|---|
| | Measured | Adjusted |
| average | 60 | 60 |
| stdev | 11.8 | 3.4 |
| band/Stdev (sigmas) | 2.54 | 8.92 |

* adjust value (ppm) =37.75+(71.255-5.4502 x pin length, mm) from linear regression analysis

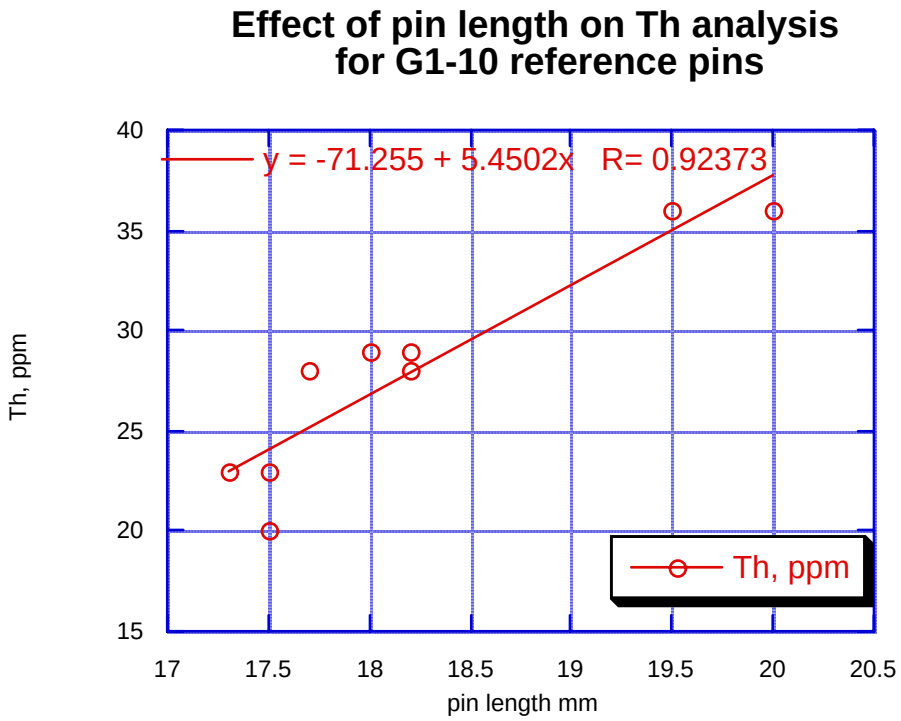


Figure 1. Linear regression analysis of thorium content versus pin length

## 2.3. CLAD VENT SET

One hundred eighteen flight quality (FQ) and 7 engineering use (EU) Clad Vent Sets (CVS) were produced in FY04. These included: 16 FQ and 1 EU CVS shipped in November 2003 for the National Aeronautics and Space Administration (NASA) Pluto/New Horizons/Enhanced Module Evaluation missions; 46 FQ long CVS were shipped to Los Alamos National Laboratory (LANL) in June 2004 and 4 EU long CVS are stored at ORNL; 39 FQ CVS were shipped for the Pluto mission in June 2004; 8 FQ and 2 EU CVS were ready to ship since July 2004 for completion of the Pluto mission; and 9 FQ CVS were completed by the end of FY04 for the NASA Multi-Mission Radioisotope Thermoelectric Generator (MMRTG) mission.

Training of a new primary dimensional inspector and a back-up welder was completed in mid FY04.

Also in mid FY04 the Power Sonics (Eldersburg, MD) ultrasonic cleaner generator (GP-1K) and tank/transducer (CT-09) had to be repaired. A spare ultrasonic generator and a tank/transducer were procured to prevent future production delays. A Gage Master model 29/GM2 comparator was refurbished by Quality Control Solutions, Inc. (Temecula, CA). It is being used for improved in-process checks for cup features (particularly vent notches).

Successful weld repairs were made on internal water leaks on both vacuum furnaces A and B. Furnace A is the primary furnace for frit vent assembly sintering and diffusion bonding operations. Furnace B is the primary furnace for cup recrystallization, decontamination cover stress relief, and vacuum outgassing operations. Vacuum levels on the low $10^{-6}$ Torr scale are being achieved at the end of furnace runs for both furnaces.

The coated steel blower for the laboratory hoods (Kewaunee Scientific Corporation, Statesville, NC) used to chemically strip and clean all CVS parts corroded to failure after 8 years of use. A new Labconco Corporation (Kansas City, MO) fiberglass blower (model 7181600) and polyvinylchloride weathercap were installed on July 23, 2004. When CVS cleaning operations resumed there was a 4 week backlog of parts to be cleaned. A back-up motor for the blower has been procured.

The ORNL shield cup assembly (SCA) production data showed that the amount the weld shield extends above the cup open end face had been to the low side of the 3.56/2.79 mm requirement. The average maximum and minimum values for the first 159 production units were 3.068 mm and 2.933 mm, respectively. Prior to FY04 production 5 out of 159 (3% rejection rate) production SCAs were below the drawing requirement. During FY04 the length of the weld shield alignment step on the weld shield tab-to-cup tooling was increased incrementally to put the weld shield length in the center of the drawing tolerance for each of the 3 production fixtures. The total alignment step depth increase ranged from 0.006” to 0.009” depending on the fixture and the specific location. The average maximum and minimum values for the 11 production units welded since the final alignment step depth adjustments are 3.286 mm and 3.151 mm, respectively. The

changes can be seen graphically in Chart 1 where the 11 values on the right side of the chart are much more centered between the specified 3.56 mm maximum and 2.79 mm minimum. This feature will be monitored during future production.

**Chart 1. ORNL Shield Cup Assembly Length from -A- (2.79/3.56 mm)**

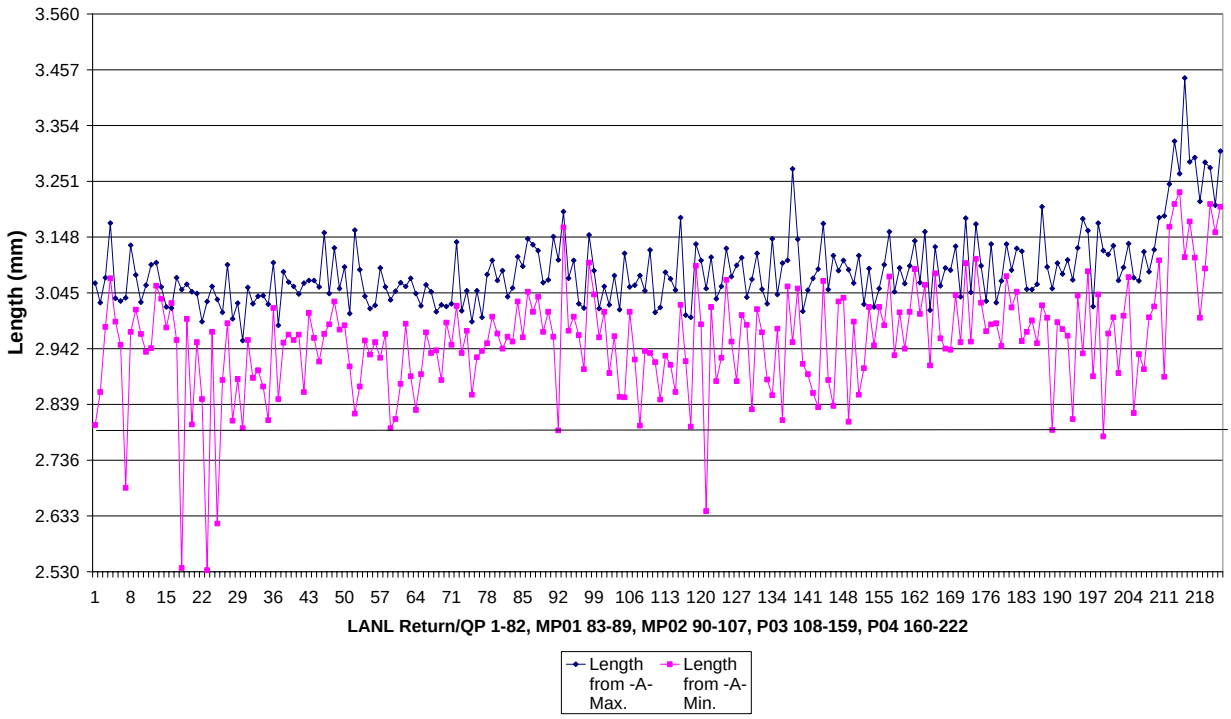


The following deviation requests were submitted and accepted during FY04:

DR-CVS-047 - revised specification GPHS-M-189 to revision E to allow a maximum of 0.40 weight percent iron in tungsten carbide grit blast powder,

DR-CVS-048 - revised procedure GPHS-Y-021 to revision G to allow the use of an additional carbon analyzer, LECO model CS400, for analyzing carbon in iridium,

DR-CVS-049 - revised procedure GPHS-XF-3619 to revision L to more accurately describe the decontamination cover fabrication process and modify use of the forming lubricant,

DR-CVS-050 - revised procedure GPHS-C-3624/25 to revision U to allow use of a coordinate measuring machine in addition to an optical comparator for measuring cup diameters,

DR-CVS-051 - revised all 10 foil fabrication and inspection procedures to streamline the part container labeling requirements and updated the middle 2 digits (insert number) of the 10 digit part numbers.

The following nonconformance reports were submitted and accepted during FY04:

NCR-CVS-042 – vent cup assembly (VCA) 9753-31-4093 was downgraded to EU because of black spots in the weld zone,

NCR-CVS-043 – VCA 9753-31-4103 was downgraded to EU after electron beam weld tooling compression post impacted the inside bottom of the cup after a 2 inch free fall,

NCR-CVS-044 – vent cups 3624-31-4118 and -4139 were downgraded to EU after being dropped 10 inches and 3.5 feet, respectively, during dye penetrant inspection,

NCR-CVS-045 – SCA 9754-05-5143 maintained FQ status with minimum weld shield length from datum -A- only 0.01 mm below the minimum drawing requirement,

NCR-CVS-046 – vent cups 3624-31- 4134 and -4135 were downgraded to EU because of minimum radius thicknesses below the 0.55 mm minimum,

NCR-CVS-047 – vent cups 3624-31-4113 and -4114 were downgraded to EU with heights below the minimum height requirement of 15.04 mm and inside depths below the minimum inside depth requirement of 14.36 mm. Cup 4114 also was out-of-flat,

NCR-CVS-048long – long vent cups 3624-lgeu-V506, -V521, -V538, and –V540 and long shield cups 3625-lgeu-S008, -S015, -S030 were downgraded to EU with heights below the minimum height requirement of 17.58 mm and inside depths below the minimum inside depth requirement of 16.90 mm. Also the minimum radius thickness for S008 was below 0.48 mm minimum. Additionally cup 3625-lgeu-S028 was downgraded to EU with a minimum diameter in the closure weld zone below the 29.73 mm minimum requirement,

NCR-CVS-049long – long VCA 9753-lgeu-V521, long SCAs 9754-lgeu-S008, -S015, and -S030, and long matched assemblies 9808-lgeu-M047 and -M048 were downgraded to EU for short inside depths/heights. These assemblies were made from cups dispositioned previously on NCR-CVS-048long,

NCR-CVS-050 – vent cup 3624-05-4180 was first-formed without a grafoil lubricant disc. Prior to weld repair of the torn stainless steel sidewall the cup was dropped 2 feet onto a synthetic tile floor. The cup maintained FQ status when all inspection requirements were met,

NCR-CVS-051 – shield cup 3625-31-5169 was downgraded to EU because it was ground and lapped too short,

NCR-CVS-052 – vent cup 3624-05-4156 maintained FQ status because the minimum height was only 0.01 mm below the 15.04 mm minimum height requirement and it was corrected subsequently during the VCA straightening operation. This occurred as a result of having to re-grit blast and re-scribe because the original scribed identity was improperly positioned.

NCR-CVS-053long - long VCA 9753-lgeu-V538 was downgraded to EU (in addition to that described on NCR-CVS-048long) for frit vent-to-cup weld problems as well as for a delamination remnant found during a scanning electron microscopy surveillance of the closure weld zone,

NCR-CVS-054 – VCAs 9753-05-4165 and -4166 were rejected for any use except as set-up hardware because of intermittent excessive weld penetration during the frit vent-to-cup welding operation. This was later attributed to malfunctioning Action Pak® signal conditioners. These signal conditioners have been repaired.

There were 6 more NCRs (NCR-CVS-055 through -060) pending for cups fully processed in FY04 (some of these actually completed in early FY05). These NCRs involved 15 more cups. This means there were 37 nonconforming cups (not assemblies) out of a total of 366 cups processed in FY04. Excluding the nine cups that were used for the required heat treat lot destructive testing, 320 out of 357 cups or 90% were processed without NCRs in FY04.

During FY04 127 vent cup assemblies were processed. Six vent cup assemblies had nonconformances originating from the vent cup assembly process (as opposed to a cup nonconformance that carried through the vent cup assembly process and required another NCR). This means 121 out of 127 vent cup assemblies or 95% were processed without NCRs in FY04.

There were 113 shield cup assemblies processed in FY04. Only one shield cup assembly had a nonconformance originating from the shield cup assembly process (as opposed to a cup nonconformance that carried through the shield cup assembly process and required another NCR). Thus, 112 out of 113 shield cup assemblies or 99% were processed without NCRs in FY04.

In FY04 125 matched assemblies were processed without any nonconformances originating from the matched assembly process (as opposed to a cup, vent cup assembly, or shield cup assembly nonconformance that carried through the matched assembly process and required another NCR). Therefore, 125 out of 125 matched assemblies or 100% were processed without NCRs in FY04.

The summary data for FY04 FQ standard-length CVS production hardware (from milestones 2.C.1, 2.C.4, and 2.C.5) are shown in Tables 1 through 9. Tables 1 through 5 for decontamination covers, weld shields, frit vent backing discs, frit vent cover discs,

and frit vent assemblies, respectively, include all FY04 production because long cup production utilized the same foil part configurations as standard-length CVS production. The number of parts used to comprise the data is shown in the upper right of each table. The weld shield, frit vent backing disc, and frit vent cover disc are sampled for dimensional inspection except for the weld shield burn back feature which is measured on 100% of the parts. The items with boxes around them are ± 3 sigma (standard deviation) limits that are outside the attribute requirements. These attributes will be monitored closely during future production to determine if and/or when production tooling should be modified.

**Table 1. FY04 FQ Decontamination Production Data -181 parts**

| Attribute/Requirement (mm) | Average | Std. Dev. | Minimum | Maximum | -3 Sigma Limit | + 3 Sigma Limit |
|---|---|---|---|---|---|---|
| Diameter max - 11.6 | 11.561 | 0.012 | 11.522 | 11.584 | 11.525 | 11.597 |
| Diameter min - 11.5 | 11.531 | 0.013 | 11.502 | 11.570 | 11.493 | 11.569 |
| Outside sph. radius max - 6.6 | 6.054 | 0.071 | 5.518 | 6.184 | 5.841 | 6.266 |
| Outside sph. radius min - 5.5 | 6.023 | 0.066 | 5.512 | 6.110 | 5.824 | 6.221 |
| 1.5 min to blend radius - max | 1.796 | 0.104 | 1.592 | 2.002 | 1.485 | 2.107 |
| 1.5 min to blend radius - min | 1.710 | 0.089 | 1.548 | 1.858 | 1.442 | 1.979 |
| Height 1.40/1.14 | 1.224 | 0.018 | 1.184 | 1.275 | 1.171 | 1.276 |
| Wall thickness max - 0.16 | 0.131 | 0.006 | 0.119 | 0.151 | 0.112 | 0.150 |
| Wall thickness min - 0.10 | 0.125 | 0.007 | 0.113 | 0.148 | 0.104 | 0.145 |
| Leak rate max - 1.0E-06 std. cc/s | 2.45E-09 | 1.55E-09 | 1.00E-09 | 1.00E-08 | 0 | 7.10E-09 |

**Table 2. FY04 FQ Weld Shield Production Data - 22/162 parts**

| Attribute/Requirement (mm) | Average | Std. Dev. | Minimum | Maximum | -3 Sigma Limit | +3 Sigma Limit |
|---|---|---|---|---|---|---|
| Total length max - 87.99 | 87.937 | 0.023 | 87.896 | 87.985 | 87.868 | 88.007 |
| Total length min - 87.88 | 87.921 | 0.026 | 87.890 | 87.972 | 87.844 | 87.998 |
| Width (no tab) max - 6.60 | 6.403 | 0.028 | 6.366 | 6.463 | 6.320 | 6.486 |
| Width (no tab) min - 6.10 | 6.335 | 0.058 | 6.250 | 6.424 | 6.162 | 6.508 |
| Tab width max - 8.38 | 8.148 | 0.052 | 8.058 | 8.232 | 7.994 | 8.303 |
| Tab width min - 7.90 | 8.110 | 0.062 | 7.988 | 8.201 | 7.922 | 8.297 |
| Tab breadth max - 2.80 | 2.581 | 0.015 | 2.550 | 2.608 | 2.537 | 2.626 |
| Tab breadth min - 2.28 | 2.568 | 0.019 | 2.542 | 2.606 | 2.512 | 2.623 |
| Length to 1st tab - 14.73/14.58 | 14.652 | 0.021 | 14.606 | 14.694 | 14.589 | 14.714 |
| Length to 2nd tab - 44.04/43.89 | 43.962 | 0.023 | 43.922 | 44.002 | 43.894 | 44.030 |
| Length to 3rd tab - 73.35/73.20 | 73.281 | 0.020 | 73.236 | 73.322 | 73.220 | 73.341 |
| Thick max - 0.160 | 0.139 | 0.007 | 0.121 | 0.151 | 0.118 | 0.159 |
| Thick min - 0.100 | 0.133 | 0.007 | 0.111 | 0.148 | 0.111 | 0.154 |
| Burnback max - 0.64 | 0.421 | 0.135 | 0.078 | 0.632 | 0.016 | 0.825 |

**Table 3. FY04 FQ Frit Vent Backing Disc Production Data - 37 parts**

| Attribute/Requirement (mm) | Average | Std. Dev. | Minimum | Maximum | -3 Sigma Limit | +3 Sigma Limit |
|---|---|---|---|---|---|---|
| Outside diameter max - 9.61 | 9.577 | 0.012 | 9.550 | 9.600 | 9.543 | 9.612 |
| Outside diameter min - 9.54 | 9.563 | 0.010 | 9.546 | 9.588 | 9.533 | 9.594 |
| Inside diameter max - 1.07 | 1.031 | 0.007 | 1.020 | 1.046 | 1.011 | 1.051 |
| Inside diameter min - 0.96 | 1.023 | 0.005 | 1.014 | 1.034 | 1.008 | 1.038 |
| Positional tolerance MMC - 0.25 | 0.100 | 0.040 | 0.018 | 0.164 | 0.000 | 0.221 |
| Thickness max - 0.16 | 0.132 | 0.006 | 0.123 | 0.154 | 0.114 | 0.149 |
| Thickness min - 0.10 | 0.128 | 0.005 | 0.119 | 0.138 | 0.114 | 0.142 |

**Table. 4 FY04 FQ Frit Vent Cover Disc Production Data - 38 Parts**

| Attribute/Requirement (mm) | Average | Std. Dev. | Minimum | Maximum | -3 Sigma Limit | +3 Sigma Limit |
|---|---|---|---|---|---|---|
| Outside diameter max - 9.61 | 9.599 | 0.009 | 9.572 | 9.614 | 9.571 | 9.627 |
| Outside diameter min - 9.54 | 9.585 | 0.007 | 9.568 | 9.602 | 9.564 | 9.606 |
| Slot outer diameter max - 7.53 | 7.479 | 0.008 | 7.466 | 7.498 | 7.456 | 7.503 |
| Slot outer diameter min - 7.41 | 7.467 | 0.006 | 7.454 | 7.480 | 7.448 | 7.486 |
| Slot inner diameter max - 6.40 | 6.357 | 0.005 | 6.348 | 6.370 | 6.343 | 6.372 |
| Slot inner diameter min - 6.30 | 6.346 | 0.008 | 6.322 | 6.358 | 6.323 | 6.369 |
| Thickness max - 0.16 | 0.136 | 0.010 | 0.125 | 0.156 | 0.107 | 0.165 |
| Thickness min - 0.10 | 0.132 | 0.007 | 0.123 | 0.151 | 0.111 | 0.152 |

**Table 5. FY04 FQ Frit Vent Assembly Production Data - 153 parts**

| Attribute/Requirement | Average | Std. Dev. | Minimum | Maximum | -3 Sigma Limit | + 3 Sigma Limit |
|---|---|---|---|---|---|---|
| Powder weight 0.072/0.073 (g) | 0.0725 | 0.0002 | 0.0720 | 0.0729 | 0.0719 | 0.0731 |
| Initial thickness (mm) | 0.403 | 0.014 | 0.378 | 0.450 | 0.361 | 0.445 |
| Final thickness 0.41 (mm) | 0.389 | 0.010 | 0.364 | 0.410 | 0.359 | 0.420 |
| Initial flow rate (cc/min) | 9.74 | 4.07 | 4.75 | 30.61 | 0.00 | 21.95 |
| Final flow rate 4.5/7.5 (cc/min) | 6.18 | 0.56 | 4.75 | 7.11 | 4.51 | 7.86 |
| Maximum compression (psi) | 952 | 574 | 0 | 1600 | 0 | 2674 |
| Final weight (g) | 0.444 | 0.011 | 0.412 | 0.465 | 0.412 | 0.476 |

## Table 6. FY04 FQ Vent/Shield Cup Production Data - 252 parts

| Attribute/Requirement (mm) | Average | Std. Dev. | Minimum | Maximum | -3 Sigma Limit | + 3 Sigma Limit |
|---|---|---|---|---|---|---|
| Weld zone diameter max - 29.88 | 29.814 | 0.011 | 29.787 | 29.855 | 29.781 | 29.847 |
| Weld zone diameter min - 29.73 | 29.786 | 0.013 | 29.739 | 29.814 | 29.748 | 29.825 |
| Remainder diameter max - 29.82 | 29.776 | 0.010 | 29.745 | 29.806 | 29.747 | 29.805 |
| Remainder diameter min - 29.60 | 29.755 | 0.010 | 29.700 | 29.777 | 29.726 | 29.785 |
| Radius max - 5.96 | 5.810 | 0.011 | 5.784 | 5.865 | 5.776 | 5.845 |
| Radius min - 5.68 | 5.774 | 0.015 | 5.697 | 5.807 | 5.729 | 5.818 |
| Height max - 15.12 | 15.088 | 0.014 | 15.048 | 15.120 | 15.048 | 15.129 |
| Height min - 15.04 | 15.069 | 0.014 | 15.040 | 15.107 | 15.028 | 15.110 |
| Vent notch depth - 0.20/0.15 | 0.174 | 0.012 | 0.144 | 0.200 | 0.138 | 0.210 |
| Vent notch width - 0.40/0.50 | 0.464 | 0.019 | 0.406 | 0.496 | 0.408 | 0.521 |
| Wall thickness minimum - 0.55 | 0.590 | 0.016 | 0.550 | 0.700 | 0.542 | 0.639 |
| Weld zone wall thickness max - 0.73 | 0.711 | 0.012 | 0.680 | 0.730 | 0.674 | 0.748 |
| Weld zone wall thickness min - 0.63 | 0.683 | 0.013 | 0.642 | 0.720 | 0.644 | 0.722 |
| Roundness maximum - 0.08 | 0.031 | 0.010 | 0.014 | 0.073 | 0.000 | 0.062 |
| Flatness maximum - 0.013 | 0.006 | 0.005 | 0.001 | 0.070 | 0.000 | 0.020 |
| Surface finish max - 3.2 um | 1.818 | 0.205 | 1.140 | 2.370 | 1.204 | 2.432 |
| Surface finish min - 0.8 um | 1.299 | 0.199 | 0.940 | 1.900 | 0.703 | 1.895 |
| Character depth maximum - 0.01 | 0.006 | 0.001 | 0.004 | 0.008 | 0.002 | 0.011 |
| Inside depth max - 14.49 | 14.429 | 0.017 | 14.380 | 14.480 | 14.378 | 14.480 |
| Inside depth min - 14.36 | 14.416 | 0.018 | 14.370 | 14.470 | 14.361 | 14.471 |
| Vent hole diameter max - 0.51 | 0.480 | 0.015 | 0.424 | 0.504 | 0.436 | 0.524 |
| Vent hole diameter min - 0.38 | 0.467 | 0.015 | 0.408 | 0.498 | 0.423 | 0.512 |
| Vent hole true position MMC - 0.25 | 0.121 | 0.050 | 0.016 | 0.234 | 0.000 | 0.271 |

## Table 7. FY04 FQ Vent Cup Assembly Production Data - 76 parts

| Attribute/Requirement (mm) | Average | Std. Dev. | Minimum | Maximum | -3 Sigma Limit | +3 Sigma Limit |
|---|---|---|---|---|---|---|
| Inside depth max - 14.10 | 14.027 | 0.022 | 13.970 | 14.080 | 13.962 | 14.092 |
| Inside depth min - 13.95 | 14.009 | 0.023 | 13.960 | 14.070 | 13.940 | 14.078 |
| DC true position MMC - 0.76 | 0.121 | 0.055 | 0.008 | 0.312 | 0.000 | 0.287 |
| FV true position MMC - 0.76 | 0.270 | 0.147 | 0.028 | 0.704 | 0.000 | 0.712 |
| Post FVA weld depth (in) | 0.548 | 0.001 | 0.544 | 0.549 | 0.545 | 0.551 |
| Post DC weld depth (in) | 0.542 | 0.001 | 0.536 | 0.544 | 0.538 | 0.545 |
| Post straighten depth - .549/.555 (in) | 0.552 | 0.001 | 0.550 | 0.554 | 0.549 | 0.556 |
| Change in depth straighten-dc (in) | 0.011 | 0.001 | 0.007 | 0.016 | 0.006 | 0.015 |
| Straightening gauge reading (in) | 0.012 | 0.001 | 0.009 | 0.017 | 0.009 | 0.016 |
| Maximum straightening force (psi) | 408 | 24 | 310 | 465 | 335 | 481 |
| Final cert leak rate max - 1.0E-6 (std cc/s) | 4.64E-09 | 4.76E-09 | 1.00E-09 | 2.60E-08 | 0 | 1.89E-08 |
| VCA flow rate 4.5/7.5 (cc/min) | 5.79 | 0.67 | 4.54 | 6.96 | 3.77 | 7.81 |
| FVA flow rate 4.5/7.5 (cc/min) | 6.21 | 0.56 | 5.05 | 7.11 | 4.51 | 7.90 |
| FVA-VCA flow rate differences (cc/min) | 0.42 | 0.31 | -0.14 | 1.14 | -0.50 | 1.33 |
| Absolute value of FVA-VCA flow rate differences (cc/min) | 0.43 | 0.29 | 0.02 | 1.14 | -0.43 | 1.29 |

## Table 8. FY04 FQ Shield Cup Assembly Production Data - 64 parts

| Attribute/Requirement (mm) | Average | Std. Dev. | Minimum | Maximum | -3 Sigma Limit | + 3 Sigma Limit |
|---|---|---|---|---|---|---|
| Length from -A- max - 3.56 | 3.141 | 0.092 | 3.013 | 3.442 | 2.864 | 3.417 |
| Length from -A- min - 2.79 | 3.021 | 0.103 | 2.792 | 3.289 | 2.712 | 3.331 |
| Inside diameter min - 27.71 | 27.805 | 0.015 | 27.760 | 27.810 | 27.761 | 27.849 |
| Inside depth from -A- max - 14.49 | 14.436 | 0.031 | 14.370 | 14.487 | 14.343 | 14.529 |
| Inside depth from -A- min - 14.36 | 14.403 | 0.026 | 14.360 | 14.466 | 14.325 | 14.481 |
| Parallel to -A- max - 0.63 | 0.154 | 0.075 | 0.038 | 0.380 | 0 | 0.380 |
| Outer diameter max (info only) | 28.186 | 0.038 | 28.105 | 28.306 | 28.071 | 28.302 |
| Outer diameter min (info only) | 28.096 | 0.037 | 28.010 | 28.192 | 27.985 | 28.207 |

## Table 9. FY04 FQ Matched Assembly Production Data - 75 parts

| Attribute/Requirement (mm) | Average | Std. Dev. | Minimum | Maximum | -3 Sigma Limit | + 3 Sigma Limit |
|---|---|---|---|---|---|---|
| Inside height max - 28.59 | 28.465 | 0.035 | 28.390 | 28.533 | 28.361 | 28.570 |
| Inside height min - 28.32 | 28.412 | 0.029 | 28.350 | 28.474 | 28.325 | 28.499 |
| Radial variation max - 0.13 | 0.044 | 0.016 | 0.020 | 0.084 | 0 | 0.093 |
| Weld gap max - 0.051 | 0.026 | 0.011 | 0.005 | 0.049 | 0 | 0.059 |
| Weight (g) | 54.094 | 0.513 | 53.140 | 55.280 | 52.555 | 55.633 |

2.3.1 Complete Production and Ship 16 Flight Quality CVS for the Pluto/New Horizons/Enhanced Module Missions by November 2003

Cup and assembly processing for 16 matched assemblies was completed in early FY04. These matched assemblies shipped to LANL for the NASA Pluto New Horizons mission in November 2003.

An erratic electron beam deflection phenomenon was encountered during weld shield-to-cup welding for these early FY04 units. Degaussing of the weld shield tab-to-cup tooling (T2E800505A008, Rev. A) eliminated the deflection problem. The beam deflection appears to have been from magnetic coupling of the permanent magnets in the DC motor used to rotate the cups during welding with the stainless steel pins and screws in the weld shield tab-to-cup tooling. Certified austenitic stainless steel pins and screws were procured. The new non-magnetic screws replaced the existing magnetic screws, however, the new pins were somewhat magnetic and thus, were not used. Additional beam deflection problems were not encountered during the remainder of FY04.

2.3.2 Produce and ship 21 long clad vent sets by June 2004

2.3.3 Produce and ship 23 long clad vent sets by June 2004

A Special Instruction Deviation Request (SIDR-CVS-005), 9 modified procedures and a Long Clad Vent Set Manufacturing Document Index and Flow Sheets were written to provide configuration control of the long CVS hardware. These documents were approved by DOE NE-50 on 12/16/03. Production of long iridium alloy CVS cups began in January 2004 with the initiation of 104 FQ blank assemblies. Foil component fabrication utilized the standard CVS production processes and configuration control.

One hundred longer shipping sleeves were fabricated from high density polyethylene rods and 350 longer polypropylene containers were procured to accommodate packaging of the longer matched assemblies. The materials were evaluated by scanning electron microscopy and energy dispersive spectroscopy and were found to be acceptable for use. The sleeves were machined, ultrasonically cleaned in Micro detergent solution at room temperature ($\leq$30°C), then dimensionally inspected. Three 10-sleeve iterations of dimensional compensation were required before the final FQ yield of 99 out of 100 was achieved.

Forty six long matched assemblies were shipped to LANL on June 30, 2004. Three (2 vent and 1 shield) of the 104 cups initiated were consumed for standard heat treat lot destructive testing. Four long EU matched assemblies and 1 FQ long shield cup assembly remain stored at ORNL.

The cup, vent cup assembly, shield cup assembly, and matched assembly summary data for FQ long CVS production hardware are shown in Tables 10, 11, 12, and 13, respectively. The number of parts used to comprise the data is shown in the upper right of each table. The items with boxes around them are ± 3 sigma (standard deviation)

limits that are outside the attribute requirements. These attributes would be monitored closely during any future production to determine if and/or when production tooling should be modified.

**Table 10. FQ Long Cup Production - 93 parts**

| Attribute/Requirement (mm) | Average | Std. Dev. | Actual Min. | Actual Max. | -3 Sigma Limit | +3 Sigma Limit |
|---|---|---|---|---|---|---|
| Weld zone diameter max - 29.88 | 29.795 | 0.014 | 29.766 | 29.834 | 29.753 | 29.838 |
| Weld zone diameter min - 29.73 | 29.757 | 0.014 | 29.734 | 29.789 | 29.714 | 29.800 |
| Remainder diameter max - 29.82 | 29.748 | 0.008 | 29.729 | 29.768 | 29.726 | 29.771 |
| Remainder diameter min - 29.60 | 29.727 | 0.010 | 29.695 | 29.744 | 29.698 | 29.757 |
| Radius max - 5.96 | 5.786 | 0.021 | 5.734 | 5.839 | 5.723 | 5.849 |
| Radius min - 5.68 | 5.740 | 0.021 | 5.686 | 5.803 | 5.676 | 5.803 |
| Height max - 17.66 | 17.641 | 0.015 | 17.594 | 17.660 | 17.597 | 17.684 |
| Height min - 17.58 | 17.627 | 0.016 | 17.581 | 17.650 | 17.578 | 17.676 |
| Vent notch depth - 0.20/0.15 | 0.180 | 0.012 | 0.150 | 0.200 | 0.144 | 0.216 |
| Vent notch width - 0.40/0.50 | 0.460 | 0.019 | 0.404 | 0.496 | 0.402 | 0.518 |
| Wall thickness min - 0.55 | 0.611 | 0.015 | 0.580 | 0.640 | 0.565 | 0.657 |
| Radius wall thickness min - 0.48 | 0.509 | 0.012 | 0.480 | 0.540 | 0.472 | 0.545 |
| Weld zone wall thickness max - 0.73 | 0.694 | 0.017 | 0.640 | 0.730 | 0.643 | 0.744 |
| Weld zone wall thickness min - 0.63 | 0.665 | 0.015 | 0.630 | 0.700 | 0.619 | 0.710 |
| Roundness maximum - 0.08 | 0.048 | 0.013 | 0.017 | 0.078 | 0.009 | 0.088 |
| Flatness maximum - 0.013 | 0.003 | 0.002 | 0.001 | 0.009 | 0 | 0.008 |
| Vent hole diameter max - 0.51 | 0.480 | 0.012 | 0.442 | 0.500 | 0.445 | 0.515 |
| Vent hole diameter min - 0.38 | 0.471 | 0.012 | 0.432 | 0.490 | 0.435 | 0.507 |
| Vent hole true position - 0.25 MMC | 0.081 | 0.038 | 0.012 | 0.198 | 0 | 0.195 |
| Character depth maximum - 0.01 | 0.006 | 0.001 | 0.004 | 0.008 | 0.003 | 0.010 |
| Inside depth maximum - 17.03 | 16.997 | 0.018 | 16.940 | 17.030 | 16.943 | 17.050 |
| Inside depth minimum - 16.90 | 16.984 | 0.017 | 16.930 | 17.010 | 16.933 | 17.036 |

## Table 11. FY04 FQ Long Vent Cup Assembly Production Data - 46 parts

| Attribute/Requirement (mm) | Average | Std. Dev. | Minimum | Maximum | -3 Sigma Limit | +3 Sigma Limit |
|---|---|---|---|---|---|---|
| Inside depth max - 16.64 | 16.587 | 0.019 | 16.550 | 16.630 | 16.529 | 16.644 |
| Inside depth min - 16.49 | 16.569 | 0.020 | 16.520 | 16.610 | 16.508 | 16.630 |
| DC true position MMC - 0.76 | 0.124 | 0.061 | 0.008 | 0.258 | 0 | 0.306 |
| FV true position MMC - 0.76 | 0.280 | 0.151 | 0.024 | 0.652 | 0 | 0.732 |
| Post FVA weld depth (in.) | 0.6487 | 0.0010 | 0.6440 | 0.6500 | 0.6457 | 0.6518 |
| Post DC weld depth (in) | 0.6403 | 0.0011 | 0.6350 | 0.6420 | 0.6371 | 0.6436 |
| Post straighten depth - .649/.655 (in) | 0.6534 | 0.0007 | 0.6510 | 0.6540 | 0.6513 | 0.6556 |
| Change in depth straighten-dc (in) | 0.0131 | 0.0012 | 0.0110 | 0.0190 | 0.0094 | 0.0168 |
| Straightening gauge reading (in) | 0.0143 | 0.0007 | 0.0140 | 0.0180 | 0.0121 | 0.0164 |
| Maximum straightening force (psi) | 421 | 26 | 390 | 500 | 343 | 499 |
| Leak rate max 1.0E-6 (std cc/s) | 6.29E-09 | 3.20E-09 | 1.00E-09 | 1.20E-08 | 0 | 1.59E-08 |
| VCA flow rate 4.5/7.5 (cc/min) | 6.14 | 0.42 | 5.03 | 6.90 | 4.88 | 7.40 |
| FVA flow rate 4.5/7.5 (cc/min) | 6.21 | 0.47 | 5.07 | 6.96 | 4.82 | 7.61 |
| FVA-VCA flow rate differences (cc/min) | 0.08 | 0.22 | -0.35 | 0.61 | -0.58 | 0.73 |
| Absolute value of FVA-VCA flow rate differences (cc/min) | 0.19 | 0.13 | 0.02 | 0.61 | -0.21 | 0.58 |

## Table 12. FY04 FQ Long Shield Cup Assembly Production Data - 47 parts

| Attribute/Requirement (mm) | Average | Std. Dev. | Minimum | Maximum | -3 Sigma Limit | + 3 Sigma Limit |
|---|---|---|---|---|---|---|
| Length from -A- max - 3.56 | 3.169 | 0.115 | 2.974 | 3.433 | 2.824 | 3.515 |
| Length from -A- min - 2.79 | 3.010 | 0.100 | 2.803 | 3.263 | 2.710 | 3.310 |
| Inside diameter min - 27.71 | 27.795 | 0.031 | 27.710 | 27.810 | 27.702 | 27.888 |
| Inside depth from -A- max - 17.03 | 16.995 | 0.024 | 16.933 | 17.030 | 16.924 | 17.065 |
| Inside depth from -A- min - 16.90 | 16.950 | 0.023 | 16.907 | 16.994 | 16.881 | 17.019 |
| Parallel to -A- max - 0.63 | 0.211 | 0.124 | 0.026 | 0.618 | 0 | 0.584 |
| Outer diameter max (info only) | 28.166 | 0.029 | 28.107 | 28.228 | 28.079 | 28.253 |
| Outer diameter min (info only) | 28.059 | 0.038 | 27.990 | 28.141 | 27.944 | 28.175 |

## Table 13. FY04 FQ Long Matched Assembly - 46 parts

| Attribute/Requirement (mm) | Average | Std. Dev. | Minimum | Maximum | -3 Sigma Limit | + 3 Sigma Limit |
|---|---|---|---|---|---|---|
| Inside height max - 33.67 | 33.582 | 0.035 | 33.493 | 33.660 | 33.478 | 33.685 |
| Inside height min - 33.40 | 33.519 | 0.031 | 33.447 | 33.576 | 33.426 | 33.611 |
| Radial variation max - 0.13 | 0.051 | 0.018 | 0.015 | 0.091 | 0 | 0.106 |
| Weld gap max - 0.051 | 0.035 | 0.009 | 0.018 | 0.049 | 0.007 | 0.064 |
| Weight (g) | 59.177 | 0.308 | 58.580 | 59.810 | 58.253 | 60.101 |

2.3.4 Produce and ship 47 flight quality CVS for the Pluto/New Horizons/Enhanced Module Missions by July 2004

Thirty nine FQ CVS were shipped to LANL on June 23, 2004 for the NASA Pluto/New Horizons/Enhanced Module Evaluation missions. The remaining 8 FQ plus 2 EU CVS were ready for shipment to LANL in July 2004, however, LANL was not able to receive materials until late November 2004. These final Pluto mission CVS were received at LANL on 12/7/04.

2.3.5 Fabricate 50 flight quality CVS for the MMRTG Mission by September 2004

Fabrication of the piece parts for an additional 50 CVS for the MMRTG mission was completed by the end of FY04. Nine FQ matched assemblies were complete. Six FQ and 8 EU VCA were ready for matching. Three additional FQ VCA and 2 FQ and 1 EU SCA were ready for dimensional inspection.

Forty two frit vent assemblies, 53 decontamination covers, 40 weld shields, 32 frit vent backing discs, and 31 frit vent cover discs were ready for assembly. An additional 24 frit vent assemblies were being manufactured. Twenty eight weld shields were ready for final clean. Twenty nine decontamination covers were ready for leak testing. An additional 30 each foil parts were being fabricated.

Fifty four vent and 68 shield cups were being dimensionally inspected. Seven shield and 12 vent cups were ready for cleaning prior to grit blasting. Fourteen of these cups (8 vent and 6 shield) appeared to have been trimmed too short (<0.001 to 0.007 inches) because of a lathe travel readout error. This was caused by grime build-up on the lathe way which interfered with the mechanical pick-up for the digital readout on the lathe. These 14 cups were expected to be for engineering use only. The cup fabrication procedure was to be modified per deviation request DR-CVS-052 to prevent a recurrence.

## 2.4 IRIDIUM POWDER AND INVENTORY MANAGEMENT

The purpose of this work is to manage an iridium inventory for all heat source contractors with emphasis on the significant quantities of iridium located at Los Alamos National Laboratory and Oak Ridge National Laboratory and to maintain a no-change iridium inventory through an annual write-off of inventory and processing losses.

### 2.4.1 Iridium Demand and Supply Schedule

The attached demand and supply schedule, prepared for contingent planning purposes, presents a strategy to assess the availability of iridium for all improving and producing activities by projecting future demands. An adequate inventory needs to be maintained to meet the needs of the Pluto/New Horizons, MMRTG, and Stirling programs. The attached table indicates that enough iridium will be available for these missions.

The first part of the table shows the estimated production demand factors for flight-quality (FQ) blanks and foil. The schedule of produced blanks and foil represents the quantity and timing for delivery or storage at Oak Ridge National Laboratory (ORNL). The ingots from new material represent the quantity produced from new iridium powder to make either blanks or foil. These ingots must be produced on a timely basis to meet the lead-time requirement to produce and deliver or store the blanks and foil.

The production of the FQ blanks and foil produces recyclable iridium material that can be placed back into the production process at ORNL. A greater economic benefit is realized by using recycled material, since the need to purchase powder from an outside vendor is reduced.

Refinable iridium scrap is also generated from the production of FQ blanks, non-FQ blanks, and foil. This scrap is sent to a commercial refinery when a sufficient accumulation occurs at ORNL, funding is available for the refining, and it makes economic sense based on a comparison of refining costs to that of new material.

Process losses of iridium occur during the working of the material at ORNL and Los Alamos National Laboratory. Losses also occur during the refining process. These inventory losses are written-off annually.

Two iridium powder purchase contracts have been completed in FY 2004 as shown in the supply strategy portion of the table. The available recycle material and scrap has been considered to have been already recycled before calculating how much powder needs to be purchased.

The information contained within the table can be summarized as follows. With the completion of the two iridium powder purchase contracts in FY 2004 and a refining operation starting in FY2005, there will be adequate supply of iridium powder to produce the hardware for the three upcoming missions and 48 kg will remain at the beginning of FY 2008.

**Demand and Supply Schedule Shows Factors and Provides Strategy to Ensure an Adequate Supply of Iridium Powder for Pluto/ New Horizons, MMRTG, and Stirling Missions**

| Factors and strategy | U. S. Government fiscal years | | | |
|---|---|---|---|---|
| | FY 2004 | FY 2005 | FY 2006 | FY 2007 |
| Production-demand factors | | | | |
| Produced blanks | 293 | 280 | 150 | 50 |
| Ingots from new material | 3 | 2 | 1 | 1 |
| Ingots from recyclable material | 0 | 0 | 1 | 0 |
| Produced foil ($m^2$) | 0.4 | 0 | 0.4 | 0 |
| Refining and process losses (kg) | | | | |
| Refining loss | 0 | 0 | 9.0 | 0 |
| Processing losses | 7.5 | 4.0 | 4.0 | 4.0 |
| Supply strategy (kg)[1] | | | | |
| Beginning balance of powder | 86 | 71 | 37 | 65 |
| Receipt of refined powder | 0 | 0 | 46 | 0 |
| Receipt of purchased powder | 39 | 0 | 0 | 0 |

[1]FY 2008 beginning balance of powder is estimated to be 48 kg.

2.4.2 Annual Write-Off

The annual fiscal year 2004 write-off of iridium inventory was completed in June. A total of 7.5 kg of iridium was written off as a normal operating loss. The write-off appropriately reduced the non-fund iridium inventory. This 7.5 kg loss was considered a normal operating loss compared to the history of iridium losses during the past several years.

2.4.3 Iridium Accountability Reviews

The review at ORNL was conduced in May. The purpose of this review was to evaluate the accountability, physical inventory, and security of iridium at ORNL. It was concluded that the accountability, physical inventory, and security for the iridium was in place and operating in a proper manner. One recommendation was proposed to enhance the present accountability and physical inventory system.

The review at LANL was conduced in June. The purpose of this review was to evaluate the accountability, physical inventory, and security of iridium at LANL. It was concluded that the accountability, physical inventory, and security for the iridium was in place and operating in a proper manner. No recommendations were necessary..

2.4.4 Shipment of Iridium

The shipment of seventeen (17) clad vent sets departed ORNL on November 21 and arrived at LANL on November 25. The security seals on the shipping container were intact upon arriving at LANL. U. S. Department of Energy Transfer Voucher No. 100-OR4-AL1-118 dated January 4, 2004 was issued to properly account for this shipment.

The shipment of thirty-nine (39) clad vent sets departed ORNL on June 23 and arrived at LANL on June 24. The security seals on the shipping container were intact upon arriving at LANL. U. S. Department of Energy Transfer Voucher No. 100-OR4-AL1-119 dated July 6, 2004 was issued to properly account for this shipment.

The shipment of forty-six (46) clad vent sets departed ORNL on June 30 and arrived at LANL on July 1. The security seals on the shipping container were intact upon arriving at LANL. U. S. Department of Energy Transfer Voucher No. 100-OR4-AL1-120 dated.

# 3. ALLOY CHARACTERIZATION

## 3.1 TENSILE BEHAVIOR OF Ta-10W

### 3.1.1 Introduction

Tensile tests were conducted on Ta-10W. Yield strength, ultimate tensile strength, uniform elongation, and total elongation from room temperature to 1100C are reported for both base metal and transverse weld material.

### 3.1.2 Material

The base material for the strength member was selected as Ta-10W due to considerations of material availability and expected mechanical properties relative to design requirements. The tensile specimens (and creep) were made from 3.175 mm (0.125 in) thick plate. The plate was rolled to 2.34 mm (0.092 in) thick, sheared into 76.2-88.9 mm x 177.8 mm (3-3.5x7 $in^2$) coupons, with the 76.2-88.9 mm length parallel with the rolling direction, degreased and acid cleaned, annealed at 1427C for 1 hr, welded (at ANL-W), machined, degreased and acid cleaned, inspected, and finally tested. The chemical composition for the Ta-10W in the as-received condition is provided in Table 1 (all units in weight ppm unless noted). The specification and two measurements are provided, one from Cabot and one from Wah Chang. Note, there was no significant pick-up of interstitial elements during processing; oxygen, carbon, hydrogen and nitrogen levels were reported by Wah Chang to be < 50, < 20, < 3, and < 20 wppm.

**Table 1. Chemical Composition of Ta-10W in the As-Received Condition**

| 5-Sep-03<br>Ta-10W, 0.125" thick, Lot# 225030 | | | | | | |
|---|---|---|---|---|---|---|
| | C | N | Si | Fe | Nb | Ta |
| Cabot | 11 | <10 | 0.01 | 0.002 | 100.33 | 90.05% |
| Wah Chang | < 20 | <20 | <50 | <50 | <50 | bal |
| ORNL Met-MatP-TS-10 | 200 max | 100 max | 50 max | 100 max | 1,000 max | Bal |
| | | | | | | |
| | H | Ni | Ti | Mo | O | W |
| Cabot | <5 | 0.005 | 0.001 | 1.733 | 41 | 9.94% |
| Wah Chang | <3 | <50 | <50 | <50 | <50 | 9.74% |
| ORNL Met-MatP-TS-10 | 15 max | 100 max | 100 max | 200 max | 150 max | 9.0-11.0% |

### 3.1.3 Experimental Procedure

Tests were conducted on a MTS test frame with a stainless steel, double-walled water cooled vacuum chamber using an Instron 8500 controller and a MTS hydraulic actuator. All tests were conducted in a vacuum of 5E-6 Torr or better; typical vacuum levels were on the order of 1E-7 Torr or better. An oil-free roughing pump and a cryo-pump were used in achieving a vacuum. Test samples were cleaned with acetone and methanol, followed by acid cleaning prior to testing; standard ultra high vacuum cleanliness procedures were followed during the entire testing and sample preparation process to

avoid contamination of the samples. Test data were collected with a laptop PC equipped with a LabView program and National Instrument data acquisition hardware.

Heating of each test specimen was conducted with a 3-kW CycleDyne induction heater in conjunction with a Nb-1Zr susceptor with an alumina heat shield, controlled by a Barber Coleman 550 temperature controller. Type C thermocouples were used for temperature measurement and control. All tests were conducted under position control with a ram rate consistent with an approximate strain rate in the tensile sample of 1E-3 mm/mm/second; load was measured with a 2,500 pound load cell.

3.1.4 Test Matrix

The test matrix for the Ta-10W base metal and transverse weld samples is provided in Table 2. Several uniaxial creep tests were also conducted at 1000, 1100 and 1200$^{O}$C at stress levels of 172, 172, and 138 MPa, respectively.

**Table 2. Tensile Test Matrix of Ta-10W**

| Purpose | Sample Type | Temperature (C) | | | | | | | | | | |
|---|---|---|---|---|---|---|---|---|---|---|---|---|
| | | RT | 300 | 500 | 750 | 850 | 900 | 950 | 1000 | 1050 | 1100 | QTY |
| YS, UTS, $\varepsilon_f$ | Tensile, base metal | 1 | 1 | 1 | 1 | 1 | 0 | 1 | 0 | 0 | 1 | 7 |
| YS, UTS, $\varepsilon_f$ | Tensile, transverse weld | 1 | 0 | 0 | 1 | 1 | 0 | 1 | 0 | 0 | 1 | 5 |
| YS= yield strength, UTS=ultimate tensile strength, and $\varepsilon_f$ = strain at fracture. | | | | | | | | | | | | |

3.1.5 Ta-10W Tensile Test Results

Tables 3a and 3b provide a summary of the tensile test results on base and transverse weld Ta-10W, respectively. The tensile test results are also plotted in Figures 1a and 1b. As observed in Figure 1a, the yield and ultimate strengths decrease with temperature, almost linearly. Base metal yield and ultimate strengths are consistently higher than that of the transverse weld material. Base metal uniform elongation is good at room temperature, ~13%, decreasing gradually and saturating at about 5% near 800-900C. Weld metal uniform elongation at room temperature is significantly lower, ~ 7%; however, the weld retains most of this ductility, ~ 5%, for temperatures up to at least 950C. Uniform elongation decreases in the weld at 1100C to nearly 2.5%. Note, the total elongation (rupture strain or failure strain) follows a similar trend, except that a local minimum appears to occur near 300C and 750C. At room temperature, the weldment total elongation is nearly identical to that of the base metal uniform elongation. For elevated temperatures, weldment total elongation is consistently higher than that of base metal uniform elongation. However, weld metal total elongation decreases from 950C to 1100C, whereas that of the base metal increases. One should note, the results presented

are for single tests. Additional tests would assist in revealing the degree of variability or scatter in the test results.

**Table 3a . Tensile Test Results of Ta-10W Base Metal**

| Ta-10W Base Metal | | | | |
|---|---|---|---|---|
| Temp (C) | YS (MPa) | UTS (MPa) | Uniform Elongation (%) | Failure Strain (%) |
| 21 | 567.5 | 648.8 | 13.1 | 23.6 |
| 300 | 413.7 | 526.8 | 8.0 | 16.5 |
| 500 | 393.7 | 494.4 | 6.8 | 17.1 |
| 750 | 330.3 | 415.1 | 6.3 | 13.4 |
| 850 | 311.0 | 379.9 | 5.5 | 13.2 |
| 950 | 293.0 | 346.1 | 5.7 | 16.2 |
| 1100 | 256.5 | 291.0 | 4.8 | 20.7 |

**Table 3b. Tensile Test Results of Ta-10W Transverse Weld**

| Ta-10W Transverse Weldment | | | | |
|---|---|---|---|---|
| Temp (C) | YS (MPa) | UTS (MPa) | Uniform Elongation (%) | Failure Strain (%) |
| 21 | 521.3 | 605.4 | 6.8 | 13.9 |
| 300 | NA | NA | NA | NA |
| 500 | NA | NA | NA | NA |
| 750 | 250.3 | 368.9 | 5.1 | 10.2 |
| 850 | 242.0 | 323.4 | 5.3 | 10.6 |
| 950 | 208.9 | 295.1 | 5.4 | 11.5 |
| 1100 | 180.7 | 229.6 | 3.3 | 7.4 |

NA: not tested

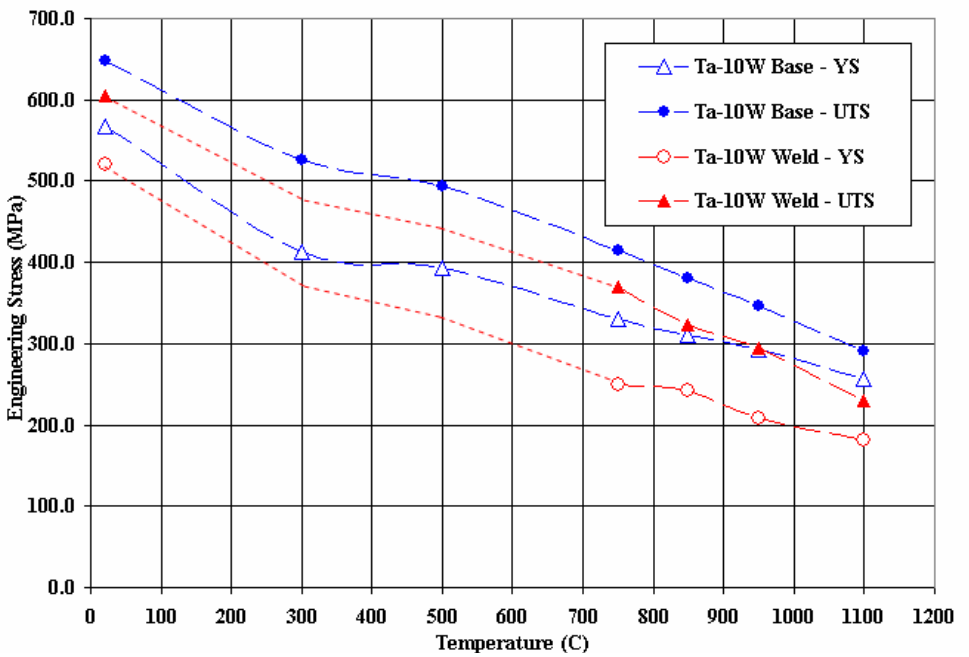


Figure 1a. Yield and Ultimate Tensile Strength Results of Ta-10W Base Metal and Transverse Weld.

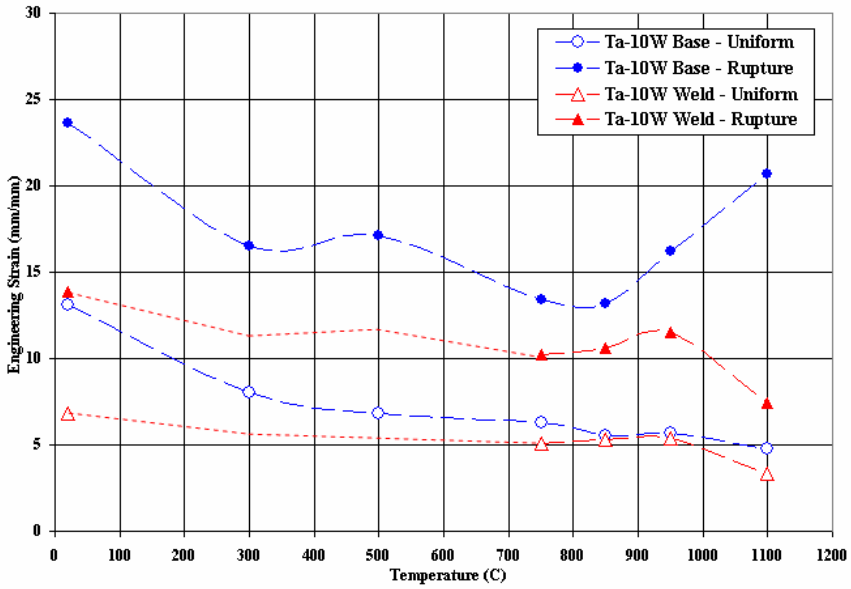


Figure 1b. Uniform and total elongation (rupture) strain results of Ta-10W base metal and transverse weld.

3.1.6 TA-10W Base Metal Uniaxal Creep Results

Several uniaxial creep tests were conducted on Ta-10W base metal. The goal was to obtain both creep rupture and time to 2% strain on a limited number of tests. Three tests were planned and are listed in Table 4.

**Table 4. Uniaxial Base Metal Creep Test Matrix**

| Test ID | Test No | Temperature (C) | Stress (ksi) | Stress (MPa) | Purpose |
|---|---|---|---|---|---|
| TCB2 | 1 | 1100 | 25 | 172 | Verify time to 2% creep & time to rupture |
| TCB4 | 2 | 1200 | 20 | 138 | Verify time to 2% creep & time to rupture |
| TCB3 | 3 | 1000 | 25 | 172 | Verify time to 2% creep |

The results for time to 2% creep are listed in Table 5. Measured times to reach 2% creep were comparable to that predicted with creep correlation obtained from data reported by Stephenson [2] when scatter in data is considered. Comparison of rupture times, seen in Table 6, revealed shorter times to rupture than that reported by Stephenson. Differences are attributed to grain size differences and annealed vs. cold-worked conditions.

**Table 5. Results of Time to 2% Creep for Ta-10W Base Metal**

| **Temperature (C)** | **Stress (ksi)** | **Stress (MPa)** | **Stephenson correlation of time 2% (hr)** | **Measured Time to 2% Creep (hrs)** |
|---|---|---|---|---|
| **1100** | **25** | **172.3** | **4** | **19** |
| **1200** | **20** | **137.8** | **2** | **37** |
| **1000** | **25** | **172.3** | **68** | **350** |

**Table 6. Creep Rupture Data of Base Metal Ta-10W**

| Temperature (C) | Stress (ksi) | Stress (MPa) | Measured Time to Rupure (hrs) | Correlation of Stephenson's Time to Rupture (hrs) |
|---|---|---|---|---|
| 1100 | 25 | 172.3 | 150 | 1,100 |
| 1200 | 20 | 137.8 | 96 | 312 |
| 1000 | 25 | 172.3 | NA | 28,743 |

3.1.7 Summary

Tensile mechanical properties of Ta-10W were measured and are consistent with those expected; transverse weld Ta-10W mechanical properties are lower than that of Ta-10W base metal. Uniaxial creep tests of base metal Ta-10W were conducted. Results of time to 2% creep and time to rupture are consistent with those expected.

3.1.8 References


1. "Tensile Behavior of Ta-10W", T.E. McGreevy & C.O. Stephens, Oak Ridge National Laboratory, Internal Program Report, August 31, 2004.

2. R.L. Stephenson, Creep-Rupture Properties of Unalloyed Tantalum, Ta-10%W and T-111 Alloys, ORNL-TM-1994, Oak Ridge National Laboratory, December 1967.


## 3.2 ALLOY DEVELOPMENT AND CHARACTERIZATION

3.2.1 Tensile Impact Ductility and Fracture Behavior of DOP-26 Iridium at 500-900°C

3.2.2 Introduction

DOP-26 iridium has been used successfully as a fuel-cladding material in radioisotope thermoelectric generators (RTGs) aboard many interplanetary spacecraft [e.g., 1]. New RTGs currently being designed for future NASA missions may have operating temperatures that are lower than in previous designs. The existing database of the tensile impact ductility of DOP-26 iridium extends down to only 800°C [2]. This study was undertaken to generate lower-temperature impact data down to 500°C.

### 3.2.3 Experimental Procedure

Dogbone-shaped tensile specimens with gage sections measuring 11.4 × 2.5 × 0.63 (mm) were machined from DOP-26 blanks that had been stress relieved for 1 h at 900°C. The surfaces of the specimen gage-sections were hand-polished with SiC paper through 600 grit, after which they were rinsed in acetone and ethyl alcohol and vacuum-annealed at 1375°C for 1 hour. Prior to tensile testing, microhardness indents were made along the specimen gage lengths using a 500-g load.

High-strain-rate tensile tests were performed at temperatures in the range 500-900°C using a specially designed gas-powered impact gun [3,4]. The bullet velocity used was 61 ± 3 m/s (which corresponds to an engineering strain rate of ~ $5 \times 10^3$ $s^{-1}$) and the specimen temperature was controlled within ± 10°C. Uniform tensile elongation (%EL), obtained by measuring the distance between pairs of microhardness indents before and after fracture and averaging the results for each specimen, was used as a measure of ductility. All the procedures described above are the same as those used in a previous study of DOP-26 iridium impact tested at higher temperatures of 800-1100°C [2]. In addition, in this study, we also measured the reduction in cross-sectional area of the specimens after fracture (%RA) as a second measure of ductility and compared its temperature dependence to that of %EL.

Fracture surfaces of selected specimens were examined in a scanning electron microscope (SEM) and the relative amounts of transgranular and intergranular fracture measured. Additionally, the shoulder (grip) sections of selected impact-tested specimens were polished, etched and examined in a light microscope to determine whether there was any sample-to-sample variation in grain size.

### 3.2.4 Results

Figure 1 show typical recrystallized microstructures of the DOP-26 specimens after the 1-h vacuum anneal at 1375°C. This is the standard recrystallization heat treatment given to the vent cups and shield cups during production, which results in a grain size of ~25 μm [5]. The grain sizes of our tensile specimens were similar, 23-24 μm, as listed in Table 1. All the impact tests were performed at this grain size, i.e., to simulate accident scenarios in which the fuel cladding has experienced no grain growth beyond the as-recrystallized grain size.

Table 2 lists the measured ductilities (elongations as well as reductions in area) for all the impact tests performed in the present study. At least 4 specimens were tested at each temperature. Table 2 also lists, for each test temperature, average values of ductility (%EL and %RA), and the corresponding standard deviations. There is good correlation between these two measures of ductility as shown in Fig. 2 which includes error bars corresponding to ± 1 standard deviation. The correlation suggests that the specimens elongate uniformly during the impact tests without significant necking occurring prior to fracture.

Associated with the above increase in ductility with increasing temperature is a change in the fracture mode of DOP-26 iridium from mostly intergranular at low temperatures, to mixed intergranular plus transgranular at intermediate temperatures, and mostly transgranular at high temperatures (Fig. 3). To quantify the relationship between ductility and fracture mode, the relative areas of transgranular and intergranular fracture were measured on fractographs such as those shown in Fig. 3. The results, plotted in Fig. 4, show that there is a direct correlation between tensile elongation and the amount of transgranular fracture: both increase in roughly the same manner with increasing temperature.

3.2.5 Discussion

Figure 5 shows the grain-size dependence of the impact ductility of DOP-26 iridium in the temperature range 800-1100°C obtained in an earlier study [2]. Three of the grain sizes in this plot (22, 27 and 33 μm) are comparable to the grain size in the current study (23-24 μm). Therefore, we can combine the results for these four grain sizes, as shown in Fig. 6, to obtain the temperature dependence of impact ductility over an extended temperature range (500-1100°C). Within experimental scatter, the impact ductilities obtained in the current study (at low temperatures) are consistent with what one would expect from an extrapolation of the earlier high-temperature data. Also, there is good agreement in the 800-900°C temperature range, where there is overlap between the two data sets.

Unfortunately, it is not possible to compare the standard deviations of the high- and low-temperature data sets because, in the earlier study [2], only one specimen was tested at each experimental condition. The only comparison that is possible is with the results of impact tests performed on DOP-26 ingots produced during the Cassini campaign [6]. While the experimental conditions for those tests (impact temperature, 980°C; heat treatment, 19-h anneal at 1500°C) were not the same as those used in the present study, it is interesting to note that the standard deviation of the Cassini impact tests (Table 3) is similar to the standard deviations of the current impact tests (Table 2).

At present, there is only one ductility requirement in the specifications for DOP-26 iridium, namely ≥ 13.5% elongation when tensile impact tested at 980°C after a heat treatment of 19 h at 1500°C. This requirement is shown in Fig. 6 by the dashed horizontal line for comparison with the impact ductilities obtained in the current study.

3.2.6 Summary and Conclusions

Tensile impact tests were performed on as-recrystallized DOP-26 iridium having a grain size of 23-24 μm at temperatures of 500-900°C and a bullet velocity of 61 m/s. The measured elongations ranged from ~8-30% over this temperature range. These ductilities are consistent with values that would be expected from an extrapolation of earlier high-temperature data obtained on DOP-26 iridium having similar grain sizes and impact tested at the same strain rate. Associated with the increase in ductility with increasing temperature is a change in the fracture mode from mostly intergranular to mostly transgranular. This trend is also similar to what was previously observed at higher impact temperatures. Since the current experiments were performed at a single (as-recrystallized) grain size, additional experiments are needed to determine the effects of grain growth on impact ductility.

**Acknowledgment**

This research was sponsored by the Office of Space and Defense Power Systems, U. S. Department of Energy, under Contract DE-AC05-00OR22725 with UT-Battelle, LLC.

**References**

1. http://saturn.jpl.nasa.gov/spacecraft/safety.cfm
2. C. G. McKamey, A. N. Gubbi, Y. Lin, J. W. Cohron, E. H. Lee, and E. P. George, *Grain Growth Behavior and High-Temperature High-Strain-Rate Tensile Ductility of Iridium Alloy DOP-26*, ORNL-6935, Oak Ridge National Laboratory, Oak Ridge, TN, April 1998.
3. C. T. Liu, H. Inouye, and A. C. Schaffhauser, Metall. Trans. A **12** (1981) 993.
4. C. T. Liu and H. Inouye, *Development and Characterization of an Improved Ir-0.3% W Alloy for Space Radioisotope Heat Sources*, ORNL-5290, Oak Ridge National Laboratory, Oak Ridge, TN, October 1977.
5. C. G. McKamey, E. H. Lee, G. B. Ulrich, J. L. Wright, and E. P. George, *Grain Growth Behavior of Iridium Clad Vent Set Cups Used in Radioisotope Thermoelectric Generators*, ORNL/TM-2002/15, Oak Ridge National Laboratory, Oak Ridge, TN, April 2002.
6. E. K. Ohriner, private communication.

## 3.3 ORNL CHARACTERIZATION OF MIN-K TE-1400

### 3.3.1 Introduction

Oak Ridge National Laboratory (ORNL) was requested to characterize the thermomechanical properties of Thermal Ceramics Min-K 1400TE material, hereafter referred to as Min-K, in support of its Multi-Mission Radioisotope Thermoelectric Generator (MMRTG) Program. Specially, ORNL was tasked with the determination of the high temperature compressive strength and stress relaxation behavior of Min-K up to 900°C in helium along with the formulation of a general model for the mechanical behavior exhibited by Min-K. Testing was to consist of general high temperature compressive mechanical testing, isothermal stress relaxation testing, and stress relaxation testing of samples exposed to a thermal gradient. Results of testing to date are summarized in this report.

The tasks defined in the original scope of work consisted of the following:

Task1. Evaluation of Min-K material in compression as a function of temperature.

This included the assessment of size and geometric effect on the distribution of compressive strength of Min-K, determination of distribution of compressive strength of Min-K as a function of temperature, and statistical analysis of monotonic compressive strength results.

Task 2. Stress Relaxation under both isothermal and gradient temperature conditions.

Task 3. Program Management and Reporting.

3.3.2 Experimental Procedures

Initial compression testing was performed at room temperature at various loading rates ranging between 5 and 500 psi/hour to determine the effect of sample size and geometry on the compressive strength of Min-K. Testing was performed using the set-up shown in Figure 1, which consists of an electromechanical testing machine (MTS Model 808) equipped with digital load and displacement controllers, computerized data acquisition, an alignment fixture, a 10 kN load cell, and a single zone furnace. A plexiglass/aluminum environmental chamber with helium flow is used for controlling the environment. Testing was performed on three sample geometries shown in Figure 2.

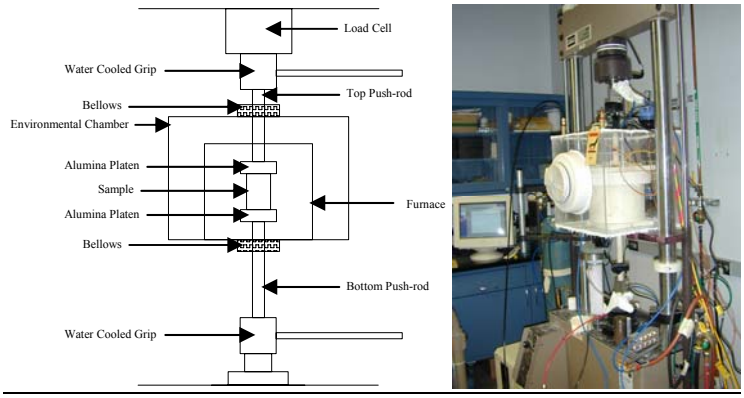


**Figure 1. Experimental set-up for determination of compressive strength of Min-K**

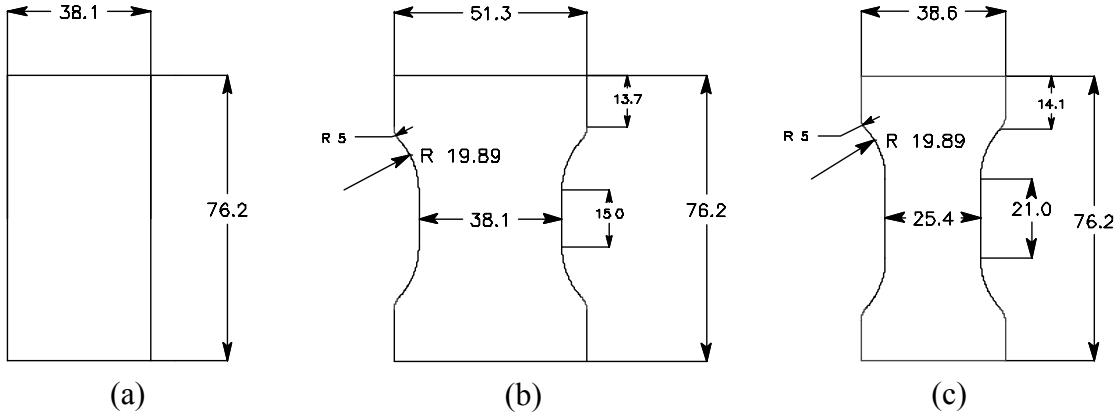


**Figure 2. Sample Geometries for Initial Compression Testing**

The results from these initial tests indicated that there was no effect of sample geometry on the monotonic compressive strength of Min-K. Therefore, subsequent testing was performed on cylindrical specimens (Figure 2.a). To determine the loading rates that would be used for stress relaxation tests, compression tests were carried out using the experimental set-up depicted in Figure 1. Testing was performed at various load rates

under load or strain control utilizing constant and step loading functions (designated fast loading (200 psi/min), nominal loading (5.56% strain/hour), and step loading (5.56% strain/hour)). Sample loading was followed by stress relaxation under strain control. Examples of testing are shown in Figure 3. Test temperatures were 900, 850, and 650°C.

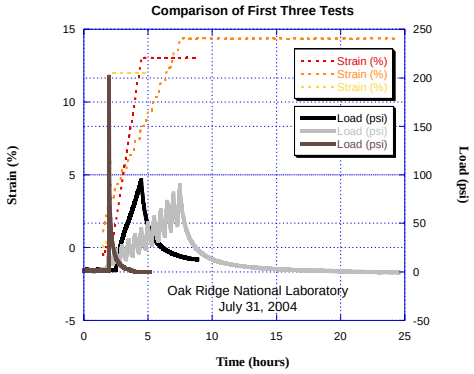


**Figure 3. Loading and Relaxation Schemes for Preliminary High Temperature Compression Testing**

Isothermal stress relaxation testing will be performed at various temperatures and loads as indicated in Table 1 using 6 inches diameter by 2 inches long cylindrical samples. Testing will be performed using the set-up shown in Figure 4, which consists of an electromechanical testing machine (Instron Mod. 1380) equipped with load and displacement analog controllers, an external LVDT for feedback displacement control, a 35 kN load cell, and a single zone furnace. A plexiglass/aluminum environmental chamber with helium flow is used for controlling the environment. Loading will be performed in strain control utilizing a 12 step loading scheme with loading every half hour at a rate of 5.56% strain/hour. Loading will be followed by stress relaxation in strain control with testing carried out until the initial load is dissipated.

**Table 1. Stress Relaxation Test Matrix**

| | Temp Profile @ 50psi | | Temp Profile @ 200psi | |
|---|---|---|---|---|
| Temp C | Gradient Sequence | Soaked Sequence | Gradient Sequence | Soaked Sequence |
| 190 | 4 (450*/190C) | 12,16 | 2 (450*/190) | 10,15 |
| 382 | - | 11,14 | - | 9,13 |
| 813 | - | 7,8 | - | 5,6 |
| 850 | 3 (850/450*) | 3,4 | 1 (850/450*) | 1,2 |

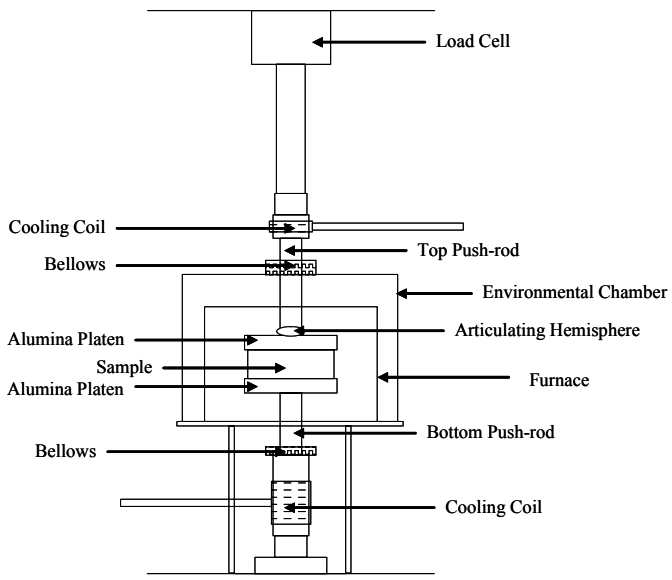


**Figure 4. Isothermal Stress Relaxation Test Frame**

Gradient stress relaxation testing will be performed at various temperatures and loads as indicated in Table 1 using 6 inches diameter, 3 inches long cylindrical samples. Testing will be performed using the set-up shown in Figure 5, which consists of an electromechanical testing machine (Instron mod. 1380) equipped with load and displacement digital controllers, a 35 kN load cell, a heated Inconel platen above the sample, and a single zone furnace. A plexiglass/aluminum environmental chamber with helium flow is used for controlling the environment. Loading will be performed in strain control utilizing a 12 step loading scheme with loading every half hour at a rate of 5.56% strain/hour. Loading will be followed by stress relaxation in strain control with testing carried out until the initial load is dissipated or has leveled off to an asymptotic value.

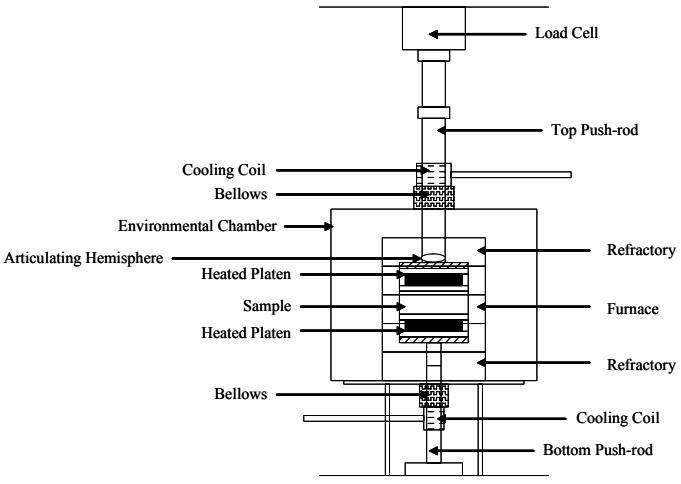


**Figure 5. Gradient Stress Relaxation Test Frame**

High temperature compression testing will be performed on cylindrical specimens (2 inches dia., 3 inches length) using the experimental set-up depicted in Figure 1. Samples

will be loaded in load control at a rate of 53 psi/hour in three load steps of 50, 100 and 200 psi with quick unload/load cycles between steps. Loading will be followed by a 3-hour hold period in load control to allow for sample creep. Testing will be carried out at 850, 813, 382, and 190$^{o}$C.

### 3.3.3 Results

Results from initial compression testing of various sample sizes and geometries are shown in Appendix 1. The key finding from this testing was that the simple cylindrical samples presented the most logical sample geometry due to the ease of sample fabrication and the simplified data analysis as compared to the hour glass sample geometries. Additionally, the data obtained using the cylindrical geometry samples was comparable to that obtained with the two hour glass geometries after correction for effects of these geometries was made (i.e. correction for neck portions of samples and non-uniform cross section of samples). This is shown in Figure 6.

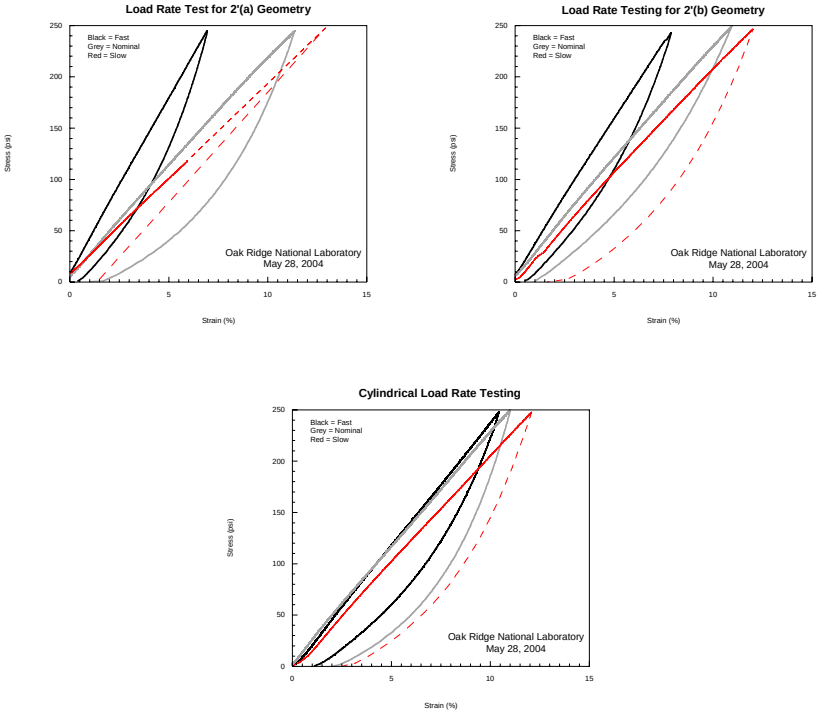


**Figure 6. Results of Initial Compression Testing**

**Results from preliminary high temperature compression testing are shown in** Figure 7. The key results from this testing were the determination of loading schemes for subsequent stress relaxation testing and high temperature compression testing. It was determined that stress relaxation samples would be loaded in strain control utilizing a 12 step loading scheme with loading every half hour at a rate of 5.56% strain/hour. High temperature compression samples will be loaded in load control at a rate of 53 psi/hour followed by a 3 hour hold in load control to allow for sample creep.

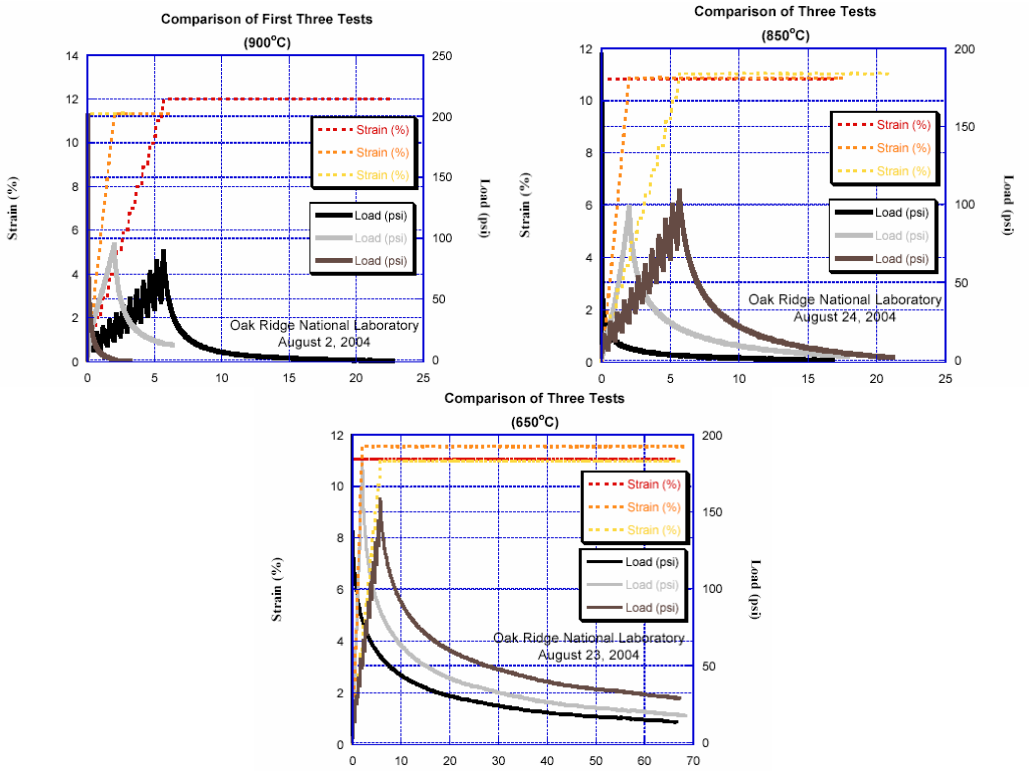


**Figure 7. Results from Preliminary High Temperature Compression Testing**

Isothermal and gradient stress relaxation testing is just getting underway. Initial results from each type of testing are shown in Figure 8 and Figure 9, respectively. Testing will continue into the next fiscal year. High temperature compression testing and model formulation is set to begin in the next fiscal year as well.

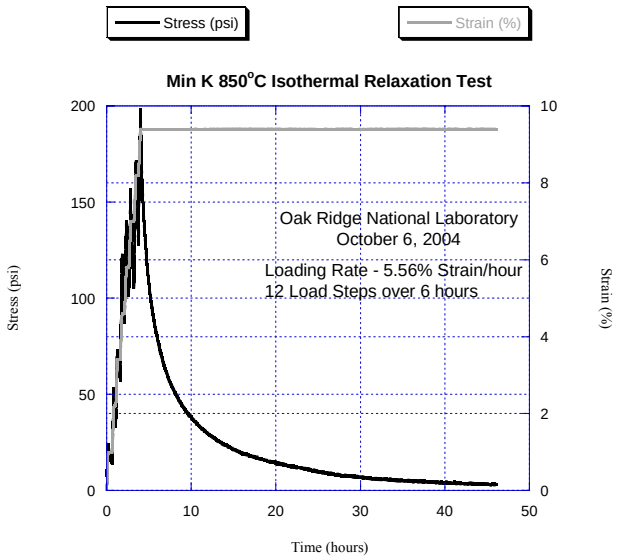


**Figure 8. Preliminary Result from Isothermal Stress Relaxation Testing**

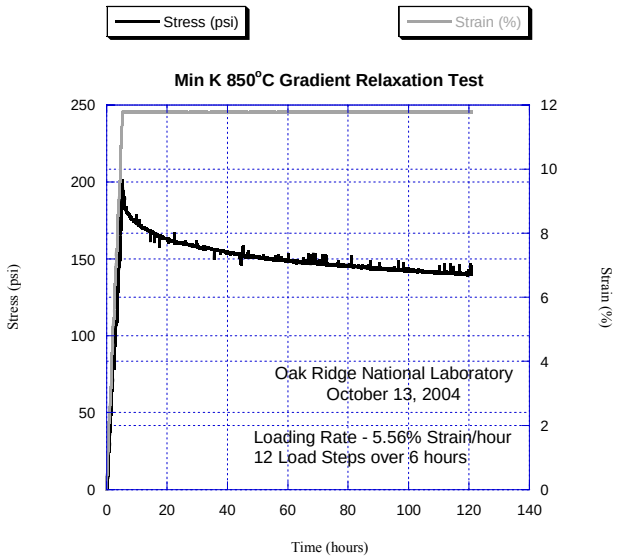


**Figure 9. Preliminary Result from Gradient Stress Relaxation Testing**

### 3.3.4 Summary

Preliminary compression testing at room temperature was performed on hour-glass and cylindrical geometry samples to determine optimum size geometry, and loading rate for subsequent testing. The key finding from this testing was that cylindrical samples were appropriate for subsequent testing due to the ease of sample fabrication and the simplified data analysis as compared to the hour glass sample geometries. Additionally, the data obtained using the cylindrical geometry samples was comparable to those obtained with the two hour glass geometries after correction for effects of these geometries was made (i.e. correction for neck portions of samples and non-uniform cross section of samples).

Preliminary high temperature compression testing was performed on cylindrical specimens (2 inches diameter, 3 inches length) to determine loading rates for subsequent testing. The key results from this testing were the determination of loading schemes for subsequent stress relaxation testing and high temperature compression testing. It was determined that stress relaxation samples would be loaded in strain control utilizing a 12 step loading scheme with loading every half hour at a rate of 5.56% strain/hour. High temperature compression samples will be loaded in load control at a rate of 53 psi/hour followed by a 3 hour hold in load control to allow for sample creep.

Five mechanical testing frames were modified to accommodate elevated temperature compression testing of Min-K samples and both isothermal and gradient-temperature stress relaxation testing in a controlled helium environment. Special heated platens were designed and constructed for the gradient-temperature stress relaxation testing. Isothermal and gradient stress relaxation testing is just being started and high temperature compression testing is set to begin in the next fiscal year. Additionally, model formulation is set to begin in the next fiscal year as well.

Appendix 1

## Min-K Testing and Characterization

Test Matrix: Preliminary Compression Tests
(Hour-Glass Specimen Geometries)

| Specimen Geometry (Dimensions in mm) | Specimen ID | Density ($lbs./in^3$) | $\sigma_y$ (psi) | E (psi) | $\varepsilon_{perm.}$ (%) |
|---|---|---|---|---|---|
| 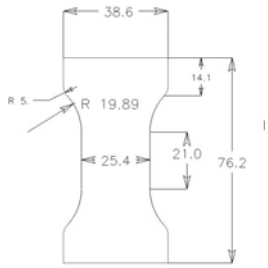  (1 inch) | 2 | 0.0124 | 109 | 2416<br>2499<br>2233 | 2.05 |
| | 12* | 0.0125 | 92 | 2424<br>2482<br>2123 | --- |
| 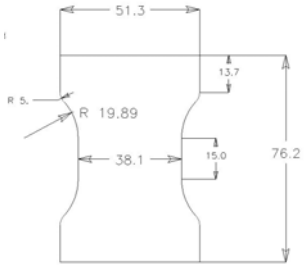  (1.5 inches) | 4** | 0.0135 | 92 | 2497<br>2256 | 0.38 |
| | 7 | 0.0134 | 103 | 2448<br>2281<br>2275 | 1.21 |

* run to very high loads (and failure) when wrong test program was used
** only run to 150 psi (2 loading cycles) before test was prematurely ended

**Min-K Testing and Characterization**
Test Matrix: Preliminary Compression Tests
(Hour-Glass Specimen Geometries)

| Specimen Geometry (Dimensions in mm) | Specimen ID | Density ($lbs./in^3$) | $\sigma_y$ (psi) | E (psi) | $\varepsilon_{perm.}$ (%) |
|---|---|---|---|---|---|
| 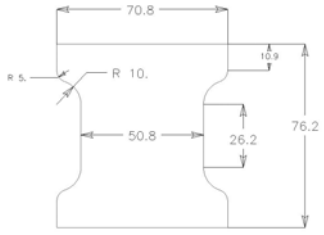 (2 inches Configuration a) | 1 | 0.0121 | 96 | 2219<br>2131<br>1984 | 1.93 |
| | 3 | 0.0123 | 96 | 1880<br>1857<br>1853 | 1.41 |
| | 5 | 0.0123 | 118 | 2259<br>2348<br>2013 | 1.46 |
| | 10 | 0.0130 | 91 | 3527<br>3370<br>3342 | 0.82 |
| | 13 | 0.0126 | 105 | 2253<br>2191<br>1885 | 0.77 |

**Min-K Testing and Characterization**
Test Matrix: Preliminary Compression Tests
(Hour-Glass Specimen Geometries)

| Specimen Geometry (Dimensions in mm) | Specimen ID | Density ($lbs./in^3$) | $\sigma_y$ (psi) | E (psi) | $\varepsilon_{perm.}$ (%) |
|---|---|---|---|---|---|
| 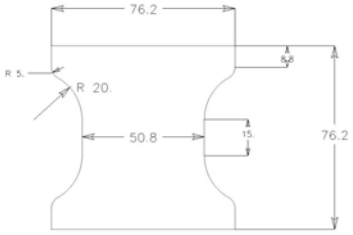 (2 inches Configuration b) | 6 | 0.0123 | 89 | 2462<br>2559<br>2180 | 1.52 |
| | 8 | 0.0124 | 95 | 2345<br>2229<br>2223 | 1.20 |
| | 9 | 0.0124 | 97 | 3168<br>2975<br>2840 | 1.24 |
| | 11 | 0.0122 | 99 | 2368<br>2196<br>2086 | 1.05 |
| | 14 | 0.0120 | 81 | 2176<br>2033<br>1933 | 1.47 |

**Min-K Testing and Characterization**

Test Matrix: Preliminary Compression Tests

(Cylindrical Specimen Geometries)

| Specimen Geometry (Dimensions in mm) | Specimen ID | Density ($lbs./in^3$) | $\sigma_y$ (psi) | E (psi) | $\varepsilon_{perm.}$ (%) |
|---|---|---|---|---|---|
| 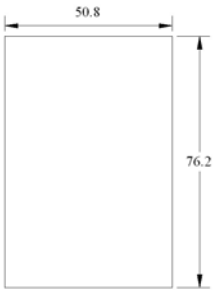 (2 inches) | 15 | 0.0132 | 99 | 2454<br>2149<br>2311 | 1.69 |
| | 16 | 0.0125 | 65 | 2401<br>2232<br>2173 | 2.05 |
| | 17 | 0.0131 | 73 | 2500<br>2358<br>2427 | 1.11 |
| | 18 | 0.0126 | 87 | 2579<br>2555<br>2004 | 2.07 |
| | 19 | 0.0132 | 76 | 2249<br>2056<br>2256 | 2.54 |